EBioMedicine 59 (2020) 102944

Contents lists available at ScienceDirect

EBioMedicine

journal homepage: www.elsevier.com/locate/ebiom

Research paper

Anti-α-synuclein ASO delivered to monoamine neurons prevents α-synuclein accumulation in a Parkinson's disease-like mouse model and in monkeys

Diana Alarcón-Arís[a,b], Rubén Pavia-Collado[a,b,#], Lluis Miquel-Rio[a,b,c,#], Valentín Coppola-Segovia[a,d], Albert Ferrés-Coy[a,b,c], Esther Ruiz-Bronchal[a,b,c], Mireia Galofré[a,b], Verónica Paz[a,b,c], Leticia Campa[a,b,c], Raquel Revilla[e], Andrés Montefeltro[e], Jeffrey H. Kordower[f], Miquel Vila[g,h,i], Francesc Artigas[a,b,c], Analia Bortolozzi[a,b,c,*]

[a] Institut d'Investigacions Biomèdiques de Barcelona (IIBB), Spanish National Research Council (CSIC), Barcelona, Spain
[b] Institut d'Investigacions August Pi i Sunyer (IDIBAPS), Barcelona, Spain
[c] Centro de Investigación Biomédica en Red de Salud Mental (CIBERSAM), ISCIII, Madrid, Spain
[d] Laboratory of Neurobiology and Redox Pathology, Department of Basic Pathology, Federal University of Paraná (UFPR), Curitiba, Brazil
[e] n-Life Therapeutics, S.L., Granada, Spain
[f] Department of Neurological Sciences, Rush University Medical Center, Chicago, IL, USA
[g] Neurodegenerative Diseases Research Group, Vall d'Hebron Research Institute, Barcelona, Spain
[h] Centro de Investigación Biomédica en Red de Enfermedades Neurodegenerativas (CIBERNED), ISCIII, Madrid, Spain
[i] Catalan Institution for Research and Advanced Studies (ICREA), Barcelona, Spain

ARTICLE INFO

Article History:
Received 17 February 2020
Revised 22 July 2020
Accepted 22 July 2020
Available online 15 August 2020

Keywords:
α-Synuclein
Antisense oligonucleotide
Axonal neurodegeneration
Dopamine neurotransmission
Mouse and monkey models
Parkinson's disease

ABSTRACT

Background: Progressive neuronal death in monoaminergic nuclei and widespread accumulation of α-synuclein are neuropathological hallmarks of Parkinson's disease (PD). Given that α-synuclein may be an early mediator of the pathological cascade that ultimately leads to neurodegeneration, decreased α-synuclein synthesis will abate neurotoxicity if delivered to the key affected neurons.
Methods: We used a non-viral gene therapy based on a new indatraline-conjugated antisense oligonucleotide (IND-ASO) to disrupt the α-synuclein mRNA transcription selectively in monoamine neurons of a PD-like mouse model and elderly nonhuman primates. Molecular, cell biology, histological, neurochemical and behavioral assays were performed.
Findings: Intracerebroventricular and intranasal IND-ASO administration for four weeks in a mouse model with AAV-mediated wild-type human α-synuclein overexpression in dopamine neurons prevented the synthesis and accumulation of α-synuclein in the connected brain regions, improving dopamine neurotransmission. Likewise, the four-week IND-ASO treatment led to decreased levels of endogenous α-synuclein protein in the midbrain monoamine nuclei of nonhuman primates, which are affected early in PD.
Conclusions: : The inhibition of α-synuclein production in dopamine neurons and its accumulation in cortical/striatal projection areas may alleviate the early deficits of dopamine function, showing the high translational value of antisense oligonucleotides as a disease modifying therapy for PD and related synucleinopathies.
Funding: Grants SAF2016-75797-R, RTC-2014-2812-1 and RTC-2015-3309-1, Ministry of Economy and Competitiveness (MINECO) and European Regional Development Fund (ERDF), UE; Grant ID 9238, Michael J. Fox Foundation; and Centres for Networked Biomedical Research on Mental Health (CIBERSAM), and on Neurodegenerative Diseases (CIBERNED).

Abbreviations: α-syn, α-synuclein; AAV-EV, adeno-associated virus empty vector; AAV5, adeno-associated virus serotype 5; ASO, antisense oligonucleotides; CPU, caudate-putamen; DA, dopamine; DAT, dopamine transporter; mPFC, medial prefrontal cortex; NET, norepinephrine transporter; PD, Parkinson's disease; SERT, serotonin transporter; shRNA, short hairpin RNA; siRNA, small interfering RNAs; SNc, substantia nigra pars compacta; TH, tyrosine hydroxylase; VTA, ventral tegmental area; h-α-synuclein, wild-type human α-synuclein

* Corresponding author.
E-mail address: analia.bortolozzi@iibb.csic.es (A. Bortolozzi).
# These authors contributed equally to the study

https://doi.org/10.1016/j.ebiom.2020.102944

Research in the context

Evidence before this study

Multiple lines of evidence support a pivotal role of α-synuclein protein in the pathogenesis of Parkinson's disease (PD). The observation that multiplication of the α-synuclein gene leads to α-synucleinopathy and neurological disease in humans is a solid premise to develop therapies that inhibit the α-synuclein overexpression. Indeed, several experimental strategies have been developed in recent years for PD using oligonucleotide therapeutics (ASO, siRNA, shRNA, etc.). However, some of them failed and even caused neuronal toxicity. A rate-limiting step for the success of oligonucleotide-based therapeutics is their delivery to the brain compartment, and once there, to selected neuronal populations.

Added value to this study

Here, we report on a newly developed indatraline-conjugated antisense oligonucleotide, IND-ASO, which reduces the synthesis of α-synuclein selectively in dopamine neurons and its accumulation in cortical/striatal projection areas over a sustained period. This is accompanied by an improvement of dopaminergic deficiencies observed in a PD-like mouse model overexpressing human α-synuclein. Importantly, this strategy does not induce the degeneration of dopamine neurons. We also reported that IND-ASO is effective in decreasing the α-synuclein protein in midbrain monoamine nuclei of nonhuman primates.

Implications of all the available evidence

Currently, there is no cure for PD and other synucleinopathies. The present therapeutic strategy based on a conjugated ASO opens the way for the selective inhibition of α-synuclein expression in PD-vulnerable monoamine neurons, resulting in a lower accumulation of reactive species of α-synuclein in anatomically connected brain regions. This study shows the benefit of the optimization of ASO molecules as a disease modifying therapy for PD and related synucleinopathies.

1. Introduction

Multiple lines of evidence support a pivotal role of α-synuclein (α-syn) protein in Parkinson's disease (PD) pathogenesis.[1] Mutations and multiplications in α-syn gene (*SNCA*) cause familial PD.[2–6] Likewise, genome-wide association studies have consistently identified common genetic variants close to the *SNCA* locus that increase the risk of idiopathic PD.[7,8] α-Syn is the major component of the intraneuronal inclusions called Lewy bodies, which accumulate extensively throughout the brain and have been suggested to underlie disease development and progression.[9] Indeed, the formation of α-syn oligomers and fibrils which are ineffectively cleared by the lysosomal or ubiquitin proteasome systems results in an aggregation and gain of toxic function of the protein and therefore, contributes to neuronal injury and degeneration.[10–13]

The observation that *SNCA* multiplication leads to α-synucleinopathy and neurological disease provides a promising approach for developing therapies that reduce α-syn expression/accumulation.[14] Gene silencing mechanisms targeting α-syn mRNA may reduce the intracellular protein content and stop/slow the progression of the illness. Preclinical studies in rodents and nonhuman primates have successfully shown that α-syn can be down-regulated in PD-affected brain areas after direct application of oligonucleotide therapeutics including antisense oligonucleotides (ASO), small interfering RNAs (siRNA) and microRNAs (miRNA).[15–23] However, one potential caveat is that in some of the animal model paradigms, a marked α-syn downregulation induced by viral vector-mediated delivery of short hairpin RNA (shRNA) displayed toxicity in nigral dopamine (DA) neurons, thus opposing the potential therapeutic effect.[24–27] Irrespectively of these potential hitches, a rate-limiting step in the development of oligonucleotide-based therapeutics is the delivery to the brain compartment, and once there, to selected neuronal populations across the lipid bilayer of the cell and endosomal membranes. In an effort to solve this problem, we recently developed conjugated oligonucleotides that selectively target genes in monoamine neurons after intranasal administration.[28] The covalent binding of monoamine transporter -SERT, DAT and NET- inhibitors (i.e., sertraline for SERT, reboxetine for NET or indatraline for all three transporters) to oligonucleotides allows their selective accumulation in serotonin, norepinephrine or DA neuronal groups after crossing the permeable olfactory epithelium and internalizing in deep Rab-7-associated vesicles.[29–32]

While many neuronal cell groups are affected in PD,[9] the illness is mainly characterised by the loss of DA neurons in the ventral midbrain and the subsequent DA deficiency in basal ganglia circuits.[33–35] In the present study, we characterised a mouse model with PD phenotype based on adeno-associated virus serotype 5 (AAV5)-mediated overexpression of wild-type human α-syn (h-α-syn) in DA neurons of substantia nigra pars compacta (SNc) and ventral tegmental area (VTA). We then attempted to reduce the h-α-syn production and found that 4 weeks after intracerebroventricular or intranasal administration of a conjugated ASO effectively suppressed α-syn synthesis in these neurons, leading to a reduced α-syn accumulation in the connected brain regions, which in term generates an improvement in DA neurotransmission. Moreover, we assessed the selectivity of a conjugated ASO-based suppression of endogenous α-syn in monoaminergic brain areas of normal aged nonhuman primate, since an age-related accumulation of α-syn protein was reported in SNc samples from human and nonhuman primates, and its prevention could be a potent therapeutic target for PD.[36–38]

2. Materials and methods

2.1. Animals

Mice. Eight-week-old wild-type male C57BL/6J mice (n = 372 for the whole study, Charles River) were housed under controlled conditions (22 ± 1°C; 12 h light/dark cycle) with food and water available *ad-libitum*. Animal procedures were conducted in accordance with standard ethical guidelines (EU directive 2010/63 of September 22, 2010) and approved by the local ethical committee (University of Barcelona).

Nonhuman primates. Eight aged rhesus macaques (four male, four female, ≥ 20 years old) were used in this study. Animals were pair-housed on a 12 h light/dark cycle with *ad-libitum* access to food and water. All procedures were approved by the Chicago Institutional Animal Care and Use Committee, Rush University (Chicago, IL), and accredited by the Association for Assessment and Accreditation of Laboratory Animal Care. Veterinarians skilled in the care and maintenance of nonhuman primates supervised animal care.

2.2. Mouse model overexpressing h-α-syn into DA neurons

Recombinant AAV5 with chicken-β-actin promoter that encodes the wild-type h-α-syn was used to overexpress h-α-syn in DA neurons of mouse SNc/VTA, as previously reported in rats.[39] The Michael J. Fox Foundation gently provided the AAV5 construct produced and tittered by the UNC Vector Core. An empty vector (AAV-EV) which noncoding stuffer DNA was also used as control group. For

stereotactic delivery of AAV5, AAV-EV or vehicle (PBS-MK: 0.26 mg/ml $MgCl_2$, 0.14 mg/ml of KCl in 1xPBS), mice were pentobarbital-anaesthetised (40 mg/kg, intraperitoneal). Volume of 1 μl of AAV5 (1.33×10^{13} gp/ml viral titter), AAV-EV or vehicle was unilaterally injected into SNc/VTA (anterior-posterior: -2.9; medial-lateral: -1.3; dorsal-ventral: -4.2 in mm)[40] using a microinjector (KDS-310-PLUS, World Precision Instruments) at 0.4 μl/min rate. The needle was kept in place for an additional 5 min before slowly being withdrawn.

2.3. Conjugated antisense oligonucleotides

Synthesis. The synthesis and purification of indatraline-conjugated ASO molecules targeting h-α-syn in AAV5 mouse model (IND-1337-ASO) or α-syn in nonhuman primate (IND-1233-ASO) as well as nonsense ASO sequence (IND-1227-ASO) were performed by nLife therapeutics S.L. as previously reported.[31] ASOs are 18-mer single stranded DNA molecules with four 2'-O-methyl RNA bases at both ends to protect the internal DNA from nuclease degradation and improve the binding to the target sequence. Sequences are IND-1337-ASO [5'-CGCCTTCCACGGTTUUCU-3'], IND-1233-ASO [5'-CUCCCTCCACTGTCUUCU-3'] and IND-1227-ASO [5′-CCGTATCGTAAG-CAGTAC-3']. In brief, ASO synthesis was performed using ultra mild-protected phosphoramidites (Glen Research) and H-8 DNA/RNA automatic synthesizer (K&A Laborgeraete GbR). Indatraline hydrochloride (triple blocker of monoamine transporters) was conjugated to 5'-carboxy-C10 modified oligonucleotide through an amide bond. This condensation was carried out under organic conditions (DIPEA/DMF, 24 h). Conjugated oligonucleotides were purified by high performance liquid chromatography using a RP-C18 column (4.6×150 mm, 5 μm) under a linear gradient condition of acetonitrile. The molecular weight of the oligonucleotide strands was confirmed by MALDI-TOF mass spectrometry (Ultra-flex, Bruker Daktronics). The concentration of conjugated sequences was calculated based on absorbance at 260 nm wavelength. Stock ASO solutions were prepared in RNAse-free water and stored at -20°C until use.

Mouse treatments. For intracerebroventricular administration, mice were pentobarbital- anaesthetised (40 mg/kg, intraperitoneal) and placed in the stereotaxic frame. A micro-osmotic pump (Alzet Model 1004, Durect Corporation) was subcutaneously implanted, while the cannula (Brain Infusion Kit 3, Alzet) was implanted in the lateral ventricle (antero-posterior -0.34, medial-lateral -1.0 and dorsal-ventral -2.2 in mm).[40] Micro-pumps were filled with IND-1337-ASO (11.36 or 37.87 mg/ml) or IND-1227-ASO (37.87 mg/ml). Alzet model 1004 osmotic pumps deliver an average infusion of 0.11 μl/h (2.64 μl/day) for 28 days, providing IND-ASO (IND-1337-ASO or IND-1227-ASO) doses of 30 μg/day (4.9 nmol/day) or 100 μg/day (16.3 nmol/day), respectively. We also added a control group that received the vehicle (2.64 μl/day). ASO doses were chosen based on previous studies showing that were secure with no signs of neuronal and glial toxicity.[31] For intranasal administration, mice were anaesthetised by 2% isoflurane inhalation and placed in a supine position.[29–32] A 5 μl-drop of phosphate buffered saline (PBS) or IND-1337-ASO was applied alternatively to each nostril once daily. A total of 10 μl of solution containing 100 μg (16.4 nmol/day) of conjugated oligonucleotides was delivered for 28 days.

Nonhuman primate treatments. Animals were reassured and then intubated on the day of surgery with ketamine (10 mg/kg, intramuscular) and propofol (2–5 mg/kg, intravenous), and placed in stereotaxic frames in the surgical suite. All surgical procedures were conducted under isoflurane anaesthesia (1–3% maintenance, inhalation) and sterile field conditions. Sufentanil (0.005–0.3 μg/kg/min, intravenous) was administered pre-operatively. Using a Medtronic Stealth Station S7 Surgical Navigation System under MRI guidance, a 22 gauge stainless steel cannula (3220P/SPC, Plastics One) was implanted into the right lateral ventricle of each animal and connected via polyethylene tubing (PE50, Plastics One) to an osmotic pump (ALZET 2ML4, DURECT Corporation) implanted subcutaneously in the animal's back. The pumps were filled with IND-1233-ASO (18.68 mg/ml) or vehicle (artificial cerebrospinal fluid 3525, Tocris Bioscience). Alzet 2ML4 osmotic pumps deliver an average infusion rate of 2.23 μl/h for 28 days, providing an IND-1233-ASO dose of 1 mg/day (163.5 nmol/day).

2.4. In situ *hybridisation*

Mice were killed by pentobarbital overdose and brains were rapidly removed, frozen on dry ice and stored at -80°C. Coronal brain sections (14 μm-thick) were obtained and processed as described elsewhere.[29–32] Antisense oligonucleotides were complementary to bases: mouse α-syn (m-α-syn, 411-447 sequence, GenBank accession NM_001042451), h-α-syn (2498-2578 sequence, NM_011430), DA transporter - DAT (564-614 sequence, NM_010020) and tyrosine hydroxylase - TH (1453-1475 sequence, NM_009377) (IBA Nucleic Acids Synthesis). Oligonucleotides were individually labelled (2 pmol) at the 3′-end with [^{33}P]-dATP (>2500 Ci/mmol; DuPont-NEN) using terminal deoxynucleotidyl-transferase (TdT, Calbiochem). For hybridisation, the radioactively labelled probes were diluted in a solution containing 50% formamide, 4x standard saline citrate, 1x Denhardt's solution, 10% dextran sulfate, 1% sarkosyl, 20 mM phosphate buffer, pH 7.0, 250 μg/ml yeast tRNA, and 500 μg/ml salmon sperm DNA. The final concentrations of radioactive probes in the hybridisation buffer were in the same range (~1.5 nM). Tissue sections were covered with hybridisation solution containing the labelled probes, overlaid with para-film coverslips and, incubated overnight at 42°C in humid boxes. Sections were washed 4 times (45 min each) in a buffer containing 0.6 M NaCl and 10 mM Tris-HCl (pH 7.5) at 60°C. Hybridised sections were exposed to Biomax-MR film (Kodak, Sigma-Aldrich, Madrid, Spain) for 1 week with intensifying screens. For specificity control, adjacent sections were incubated with an excess (50x) of unlabelled probes. Films were analysed and relative optical densities were evaluated in three adjacent sections by duplicate of each mouse and averaged to obtain individual values using a computer assisted image analyser (MCID, Mering). MCID system was also used to acquire pseudo-colour or black and white images. Figures were prepared for publication using Adobe Photoshop software (Adobe Software). Contrast and brightness of images were the only variables we adjusted digitally.

2.5. Immunohistochemistry

Mice were anaesthetised with pentobarbital and transcardially perfused with 4% paraformaldehyde (PFA) in sodium-phosphate buffer (pH 7.4). Brains were extracted, post-fixed 24 h at 4°C in the same solution, and placed in gradient sucrose solution 10–30% for 3 days at 4°C. After cryopreservation, serial 30 μm-thick sections were cut to obtain SNc, VTA and caudate putamen (CPu). Brain sections were washed and incubated in a 1x PBS/Triton 0.2% solution containing normal serum from secondary antibody host. Primary antibodies for h-α-syn (anti-h-α-syn clone Syn211 1:20; ref.: AB75305, Abcam), phospho-ser129-α-syn (anti-phospho-ser129-α-syn 1:2000; ref.: AB51253, Abcam) and TH (anti-TH 1:5000; ref.: AB112, Abcam) were used.[31] Briefly, primary antibodies were incubated overnight at 4°C, followed by incubation with the corresponding biotinylated anti-mouse IgG1 (1:200, ref.: A-10519, Life Technologies) for anti-h-α-syn, and biotinylated anti-rabbit IgG (1:200; ref.: BA-1000, Vector Laboratories) for anti-phospho-S129-α-syn and anti-TH according to the manufacturer's instructions. The color reaction was performed by incubation with diaminobenzidine tetrahydrochloride (DAB) (ref.: D5905-50TAB, Sigma-Aldrich) solution. Sections were mounted and embedded in Entellan (Electron Microscopy Sciences).

Human α-syn protein density in SNc/VTA and CPu was assessed in sections corresponding to different AP levels -2.70 to -3.80 mm and 1.1 to 0.02 mm from bregma, respectively. Sections were scanned using an Epson high-resolution scanner and sigma scan software was used to compare the relative optical density in each region of interest. Phospho-ser129-α-syn$^+$ cells were counted in the SNc/VTA using ImageJ (v1.49g). All labelled cells with its nucleus within the counting frame were counted in six consecutive SNc/VTA sections and three different microscope fields were analysed in each section. The total number of TH$^+$ cells in SNc and VTA was estimated by stereology according to the fractionator principle, using the MBF Bioscience Stereo-Investigator 11 (64 bits) Software (Micro Bright-field).[41,42] Serial 30 μm-thick sections covering the entire SNc/VTA were included in the counting procedure (every sixth section was counted for a total of 6–8 sections analysed/animal). The following sampling parameters were used: (i) a fixed counting frame with a width and length of 50 μm; (ii) a sampling grid size of 125 $\times$ 100 μm. The counting frames were placed randomly by the software at the intersections of the grid within the outlined structure of interest. The cells in one brain side, contra or ipsilateral to the injection site, were counted following the unbiased sampling rule using a $\times$ 100 lens and included in the measurement when they came into focus within the dissector. A coefficient of error of $<$0.10 was accepted. Data for the total numbers of TH$^+$ neurons in the SNc and VTA are expressed as the absolute numbers in the non-injected contralateral side and in the AAV-injected ipsilateral side.

To examine IND-1337-ASO efficacy, h-α-syn protein staining was performed on frozen 14 μm-thick sections of the midbrain from the same mice in which h-α-syn mRNA was assessed by *in situ* hybridisation. After endogenous peroxidase inhibition, pre-incubation and incubation were carried out in a 1x PBS/Triton 0.3% solution containing normal serum from secondary antibody host. The primary antibody (anti-h-α-syn clone Syn211 1:100; ref.: MA1-12874, Thermo Fisher Scientific) was incubated overnight at 4°C, followed by incubation with the biotinylated rabbit anti-sheep (1:500; ref.: BA-6000, Vector Laboratories) and subsequent incubation in ABC solution (Vector Laboratories) according to the manufactures' instructions. The colour reaction was performed by incubation with DAB solution. The sections were embedded in Entellan and investigated on a Nikon Eclipse E1000 microscope using a 40x objective. The intensity of h-α-syn labelling was quantified using ImageJ (v1.49 g) software in three equidistantly SNc/VTA sections between -2.70 to -3.80 mm from bregma for each mouse.

2.6. Confocal fluorescence microscopy

Mice were anaesthetised with pentobarbital and transcardially perfused with 4% PFA in sodium-phosphate buffer (pH 7.4). Brains were removed, and processed for confocal microscopy. After cryopreservation, serial 30 μm-thick sections were cut to obtain SNc, VTA, CPu, and motor, cingulate and visual cortices. Intracellular localisation of h-α-syn protein in TH$^+$, GFAP$^+$ or NeuN$^+$ neurons was examined by confocal microscopy using a Leica TCS SP5 laser scanning confocal microscope (Leica Microsystems Heidelberg GmbH) equipped with a DMI6000 inverted microscope, blue diode (405 nm), argon (458/476/488/496/514), diode pumped solid state (561 nm) and HeNe (594/633 nm) lasers. Brain sections were rinsed with PBS, incubated in 1% bovine serum albumin (BSA, Sigma-Aldrich), PBS/Triton 0.1% and treated with primary antibodies: anti-TH (1:1250; ref.: AB112, Abcam), anti-GFAP (1:1000; ref:Z0334, Dako), anti-NeuN (1:500; ref.: AB177487, Abcam) and anti-h-α-syn clone Syn211 (1:20; ref.: AB75305, Abcam). Sections were incubated at 4°C, rinsed and treated with secondary antibodies A555-anti-rabbit (1:500; ref.: A-31572, Life Technologies) and A488-anti-mouse IgG1 (1:500; ref.: A-21121, Life Technologies) for 120 min. Nuclei were stained with Hoechst (1:10.000, ref.: H3570, Life Technologies). Confocal images were acquired as stacks at differing 0.3 μm in the z-axis, 600Hz in a 1024 $\times$ 1024-pixel format and standard pinhole (1 Airy unit). Images were analysed and composed using ImageJ 1.49 g software. In addition, co-localization of h-α-syn and TH axons was assessed in several DA projection brain areas including CPu and, cingulate, motor (primary and secondary) and visual (primary and secondary) cortices. First, h-α-syn (green channel) and TH (red channel) labelled axonal fibre images were segmented by intensity using the automatic Li's or Otsu's threshold methods.[43,44] Particles smaller than four pixels were discarded from the final resulting images. Second, colocalised h-α-syn$^+$ and TH$^+$ axonal fibres were selected by intersection of TH axonal-segmented image and h-α-syn fibre-segmented image using the Logical AND operation (also known as Boolean AND operation) between both images to generate a new stack with only the axonal signal. Third, h-α-syn axonal swellings were defined as regions where h-α-syn protein shows a high-intensity dot pattern. Swelling regions were segmented from h-α-syn labelled fibre images using the max entropy intensity auto-threshold method.[45] Finally, area, mean intensity and integrated density were measured from total h-α-syn$^+$ fibres, TH$^+$ fibres, h-α-syn and TH labelled fibres and h-α-syn axonal swelling images.

2.7. ELISA

Mouse midbrain containing SNc/VTA was dissected out using a Mouse Brain Matrix (Ted Pella,), quickly frozen on dry ice and stored at -80°C. Maxi-Sorp plates (Thermo Nunc) containing SNc/VTA tissues were incubated with 200 ng of anti-α-syn filament antibody (The Michael J. Fox Foundation 14-6-4-2 conformation-specific, ref.: AB209538, Abcam).[46,47] Tissue samples from the rhesus macaque were processed for ELISA using Cloud-Clone Corp kit assay SEB222Mu sandwich enzyme immunoassay. Tissues were homogenised in lysis buffer (IS007, Cloud-Clone Corp) and supernatants were collected and assayed immediately. Microtiter plate has been pre-coated with an anti-α-syn clone Syn211 antibody (1:250; ref.: MS-1572, Thermo Fisher Scientific). Standards or samples were added to the appropriate microtiter plate wells with a biotin-conjugated antibody, and reaction was stopped adding 50 μl of 1N HCl per well, and absorbance was measured at 450 $\pm$ 10 nm in a Multiskan Spectrum reader (Thermo Fisher Scientific). The concentration of α-syn in the samples was determined by comparing the OD of the samples to the standard curve.

2.8. Western blot

The procedure for Western blot was as described previously.[32] Tissue samples of ventral midbrain, CPu and medial prefrontal cortex (mPFC) of mice were dissected from brain slices and homogenised in RIPA buffer (150 mM NaCl, 1% Triton X-100, 0.5% Sodium deoxycolate, 5 mM EDTA, 0.1% SDS, 50 mM Tris, pH 8.0) with protease and phosphatase inhibitors. Proteins were quantified using Pierce™ BCA Protein Assay Kit (Thermo Fisher Scientific). Protein lysate (3–15 μg) was separated using 4–15% SDS-PAGE and electro-transferred onto a nitrocellulose membrane. Protein blots were probed with primary antibodies against anti-α-syn detecting both mouse and human α-syn clone 42/α-Syn (1:1000, ref.: BD610786, BD Biosciences), specific anti-h-α-syn clone Syn211 (1:1000, ref.: MA1-12874, Thermo Fisher Scientific), anti-phospho-ser129-α-syn (1:1000, ref.: AB51253, Abcam) and, anti-β-actin (1:30000, ref.: A1978, Sigma-Aldrich) as loading control. For rhesus macaque, substantia nigra part medial was homogenised in lysis buffer (Tris-EDTA-SDS-NP40 buffer) with protease inhibitors and protein was quantified using a BCA protein assay kit (Thermo Fisher Scientific). Once proteins were electrophoresed and transferred to nitrocellulose filter membranes, they were incubated with primary monoclonal anti-α-syn clone Syn211 (1:500, ref.: 32-8100, Thermo Fisher Scientific) overnight at 4°C. Detection

was done by chemiluminescence using SuperSignal Chemiluminescence ECL substrate kit (Thermo Fisher Scientific), and pictures were taken using ChemiDoc Imaging System (Bio-Rad). Images were analysed using ImageLab software (BioRad).

2.9. In vivo *microdialysis*

Drugs and reagents. All reagents used were of analytical grade and were obtained from Merck (Darmstadt). DA hydrochloride, nomifensine maleate and quinpirole hydrochloride were from Sigma-Aldrich-RBI. D-amphetamine sulphate and veratridine were purchased from Tocris. To assess local drug effects, compounds were dissolved in artificial cerebrospinal fluid (in mM: NaCl, 125; KCl, 2.5; $CaCl_2$, 1.26 and $MgCl_2$, 1.18) and administered by reverse dialysis at the stated concentrations (uncorrected for membrane recovery).

Intracerebral microdialysis. Extracellular DA concentration was measured by *in vivo* microdialysis using high performance liquid chromatography coupled to electrochemical detection as described elsewhere.[31] One concentric dialysis probe (Cuprophan membrane; 6000 Da molecular weight cut-off; 1.5−2 mm-long) was implanted in mouse CPu (antero-posterior 0.5, medial-lateral -1.7 and dorsal-ventral -4.5 in mm) or mPFC (antero-posterior 2.2, medial-lateral -0.2 and dorsal-ventral −3.4 in mm).[40] Experiments were performed 24−48 h after surgery in freely moving mice. In an additional experiment, mice overexpressing h-α-syn and treated intracerebroventricularly with IND-1337-ASO were implanted with a guide cannula (CMA 7, ref.: CMAP000138, Harvard Apparatus) into CPu. A dummy cannula was inserted into the guide cannula to avoid contamination and fixed with screws. The day before the microdialysis experiments, the dummy cannula was removed and replaced by a 2 mm long microdialysis probe (CMA 7 microdialysis probe, ref.; CMAP000083, Harvard Apparatus). DA levels in dialysate samples were determined using high performance liquid chromatography coupled to electrochemical detection (+0.7 V, Waters 2465), with 3-fmol detection limit. The mobile phase containing 0.15 M $NaH_2PO_4.H_2O$, 0.9 mM PICB8, 0.5 mM EDTA (pH 2.8 adjusted with orthophosphoric acid), and 10 % methanol was pumped at 1 ml/min (Waters 515 HPLC pump). DA was separated on a 2.6 μm particle size C18 column (7.5 × 0.46 cm, Kinetex, Phenomenex) at 28°C.

2.10. Behavioural testing

Behavioural analyses were performed in mice at different post-AAV5 injection times thereafter (1, 4, 8, and 16 weeks) with intervals of 1−7 days between tests. Different behavioural paradigms were used to evaluate motor and cognitive functions. All tests were performed between 10:00 and 15:00 h by an experimenter blind to mouse treatments. On the test day, mice were placed in a dimly illuminated behavioural room and were left undisturbed for at least 1 h before testing.[29,30]

Cylinder test. Mice were tested for the left and right forepaw use with the cylinder test 1 week before surgery. Mice that present an asymmetry usage of the right-left forepaws at basal conditions were excluded from the analysis. Each mouse was placed in an acrylic cylinder (diameter, 15 cm; height, 27 cm), and the total number of left and right forepaw touches performed in 5 min was counted. Data are presented as the percentage of the contralateral paw usage with respect to vehicle-injected mice. Behavioural equipment was cleaned with water after each test session to avoid olfactory cues.[48]

Rotarod. Motor coordination of mice was tested on a rotarod apparatus (Letica LE8200, Panlab). This consisted of a rotating rod (3 cm-diameter; hard non-slipping plastic) divided into five 5 cm-lanes. On the same day of testing, mice were trained on the apparatus three consecutive trials in which the rod was kept at constant speed (one trial at 0 rpm and two trials at 4 rpm) for 5 min. Then, mice were placed individually for 2 consecutive trials on the rod rotating at an accelerating speed from 4 to 40 rpm in 5 min. The latency to fall of the rod and the maximal speed reached were automatically recorded.[49]

Open field test. Motor activity was measured in four Plexiglas open field boxes 35 × 35 × 40 cm indirectly illuminated (25−40 lux) to avoid reflection and shadows. The floor of the open field boxes was covered with an interchangeable opaque plastic base that was replaced for each animal. Motor activity was recorded during 15 min by a camera connected to a computer (Video-track, Viewpoint). The following variables were measured: horizontal locomotor and exploratory activity, defined as the total distance moved in cm including fast/large (speed > 10.5 cm/s) and slow/short movements (speed 3−10.5 cm/s), and the activation time.

Novelty object recognition. Mice were placed into an open field box of Plexiglas (40 × 35 × 16 cm) with an illumination (60 lux) in the centre of the box. Two objects of identical shape were used as familiar objects. During habituation period, the mice could freely explore the open field box without objects for 10 min on two consecutive days. In the acquisition test, the two identical objects were placed separately in the centre of the open field and the mice explored it for 10 min. To minimize the presence of olfactory traces, the objects and the open field were cleaned with water between each trial. 24 h after the acquisition test, one of the familiar objects was replaced by a new object and the time spend exploring of both objects (familiar and novel) was recording for a period of 10 min. The exploration of an object was defined as pointing the nose at the object at a distance of < 1 cm and/or touching it.[50]

Morris water maze. An open circular pool (70 cm in diameter, 50 cm in height) was filled halfway with water and the temperature was maintained at 22°C ± 1. Four visual clues were placed on the walls of the tank (N, E, S, and W). Non-toxic, white latex paint was added to make the water opaque, and a white escape platform was submerged 1 cm below the water level. The animals' swimming paths were recorded by a video camera mounted above the centre of the pool, and data were analysed with SMART version 3.0 software (Panlab SA). The learning phase consisted of 4 days of trials for each mouse. The animals were submitted to four trials each day which were averaged, starting from the positions set (in random order) and without a resting phase between each trial and the subsequent one. At each trial, the mouse was placed gently into the water, facing the wall of the pool, and allowed to swim for 60 s. If not able to locate the platform in this period, the mouse was guided to the platform by the investigator. Mice were left on the platform each time for 20 s in order to allow for spatial orientation. A memory test was performed at the end of the learning days, in which the platform was removed. The escape latency during the learning tasks was measured, along with the time spent in each quadrant of the pool after the removal of the platform in the probe trial.[50]

2.11. Statistical analysis

All values are expressed as the mean ± standard error of the mean (SEM). Statistical comparisons were performed using GraphPad Prism 8.01 (GraphPad software, Inc.) using the appropriate statistical tests, as indicated in each figure legend. Outlier values were identified by the Grubbs' test (i.e. Extreme Student zed Deviate, ESD, method) using GraphPad Prism software and excluded from the analysis when applicable. Differences among means were analysed by either 1- or 2-way analysis of variance (ANOVA) or two-tailed *t*-test, as appropriate. When ANOVA showed significant differences, pairwise comparisons between means were subjected to Tukey's *post-hoc* test or Sidak's multiple comparisons test as appropriate. Differences were considered significant when $P < 0.05$ (Supplemental Table 1).

2.12. Role of the funding source

Funding sources: SAF2016-75797-R, Retos-Colaboración Subprogram RTC-2014-2812-1 and RTC-2015-3309-1, Ministry of Economy and Competitiveness (MINECO) and European Regional Development Fund (ERDF), UE; Therapeutic Pipeline Program Spring 2014 Program, grant ID: 9238, The Michael J. Fox Foundation; Centro de Investigación Biomédica en Red de Salud Mental (CIBERSAM), and Centro de Investigación Biomédica en Red de Enfermedades Neurodegenerativas (CIBERNED). Role of the funding sources: generation and characterization of a PD-like mouse model, studies in monkeys, studies of the efficacy of a new PD therapy based on an indatraline-conjugated antisense oligonucleotide. Funding sources were not involved in writing, compiling, analysing, interpreting, or presenting the study, and full access to study data was provided.

3. Results

3.1. Mouse model characterization with h-α-syn accumulation in SNc/VTA

We first examined the h-α-syn transgene expression by injecting AAV5-chicken-β-actin-h-α-syn (referred to as AAV5) in the SNc/VTA of mice. The AAV5 vector was previously validated *in vivo* in rats at Dr. D. Kirik's laboratory (BRAINS Unit, Lund University).[39] To investigate the time-course of h-α-syn expression, mice were sacrificed at 1, 4, 8, and 16 weeks post-injection. Histological analysis showed that h-α-syn overexpression results in high immunoreactivity in the injected side of the midbrain (SNc and VTA), and no staining was observed on the contralateral side (Fig. 1a). Double immunofluorescent staining specific for h-α-syn confirmed that the vast majority of TH^+ neurons in SNc (~80%) and to a lesser extent in VTA (~60%) expressed the h-α-syn transgene (Fig. 1b). A modest reduction of the number of TH^+ cells in SNc (~15%), but not in VTA, distributed over the complete rostro-caudal extent were found at 8 and 16 weeks post-injection (Fig. 1c).

Using *in situ* hybridisation, we detected a progressive increase of h-α-syn, but not murine α-syn, mRNA expression in SNc/VTA compared to the control group (Fig. 1d,e and Supplemental Fig. 1). In parallel, we found that AAV5 infusion induced a marked time-dependent increase of h-α-syn protein density in ipsilateral SNc/VTA as well as CPu compared to contralateral side as assessed by immunohistochemistry (Fig. 2a and b). The maximum level of h-α-syn protein reached in SNc/VTA was found at 8 weeks after injection (260% compared to contralateral side), overlapping with the maximum number of TH^+ neurons expressing h-α-syn transgene (Fig. 1b and 2b).

Since the phosphorylation of α-syn at amino acid serine 129 (phospho-ser129-α-syn) is commonly considered an indicator for α-syn aggregation,[51–53] the signal intensity of phospho-ser129-α-syn in SNc/VTA was measured. Our data revealed that AAV5-induced h-α-syn overexpression leads to a strong and progressive α-syn phosphorylation in the ipsilateral SNc/VTA (Fig. 2c). Accumulation of phospho-ser129-α-syn began early, with positive cells being observable already at 1-week post-injection, reaching the highest levels at 8 weeks in close parallelism to h-α-syn protein accumulation (Fig. 2d and b).

Next, we performed immunoblot analysis of microdissected mouse SNc/VTA extracted 4 weeks after AAV5 injection. Western blot analysis using antibodies recognizing both murine and human α-syn as well as specific against human α-syn showed an increased monomeric α-syn protein levels in AAV5-injected mice compared to vehicle-injected group (Fig. 2e and g). Interestingly, stable forms of α-syn oligomers were also identified in AAV5 mice compared to the control group (Fig. 2f and h). Likewise, we used an additional marker for α-syn aggregation assessed by ELISA,[46,47] and detected a significant increase of oligomer α-syn levels in the ipsilateral SNc/VTA of AAV5-injected mice compared to contralateral side as well as to mice treated with vehicle (Fig. 2i).

3.2. Progressive motor and cognitive impairments in mice overexpressing h-α-syn in SNc/VTA

To determine the functional consequences of overexpressing h-α-syn in DA TH^+ neurons, we performed a time-course study to assess changes in motor and cognitive performance. Compared to vehicle-injected mice, h-α-syn overexpression induced a progressive functional deficit in the cylinder test, which was significant from 8 weeks post-AAV5 injection and maintained until 16 weeks (Fig. 3a). In addition, mice overexpressing h-α-syn in SNc/VTA also exhibited an impaired rotarod performance at 8 weeks compared to vehicle-injected mice (Fig. 3b). None of these behavioural changes was driven by changes in the spontaneous locomotor activity as assessed by the open field test (Fig. 3c). To rule out any possible effect of the vector itself we performed an experiment with an AAV-EV using exactly the same protocol that we followed for the AAV5 mice. AAV-EV injection did not alter the motor activity of mice or the expression of DA neural markers (Supplemental Fig. 2).

Mice were also tested using the novel object recognition paradigm, a behavioural task assessing short-term memory, mainly dependent on cortical areas.[54,55] During the training period, both vehicle- and AAV5-injected mice showed similar object preference, without differences between phenotypes (data not shown). In contrast, AAV5-injected mice failed to discriminate between novel and familiar objects (Fig. 3d), suggesting a deficit in short-term memory acquisition/retrieval. Moreover, we assessed the changes in spatial learning and reference memory in the Morris water maze at 4, 8, and 16 weeks post-injection. As shown in Fig. 3e, the acquisition of the task over the first 4 days of testing was impaired in AAV5-injected mice, showing significant differences in learning kinetics compared to vehicle-injected mice examined at the same time. After removal of the platform, significant changes in the time spent by mice in the target quadrant were also detected. While vehicle-injected mice preferred the target quadrant, AAV5-inject mice showed no preference for the target quadrant relative to the other three quadrants at 8 and 16 post-injection (Fig. 3e). Hence, mice overexpressing h-α-syn in midbrain DA neurons displayed an abnormal motor coordination and balance, and exhibited spatial learning and memory deficits, especially in the late phase (8 and 16 weeks post-injection). However, SNc/VTA TH^+ neurons were sufficiently resistant to the h-α-syn accumulation, suggesting that the behavioural impairments appear to be determined by the long-term persisting neuropathology in DA neurons rather than by neurodegeneration.[56]

3.3. Axonal changes induced by overexpression of h-α-syn in SNc/VTA

Next, we examined the neuropathology changes induced by local h-α-syn overexpression in midbrain DA neurons. Most striking changes occurred in DA axonal projections to anatomically connected brain regions. Despite the modest loss of TH^+ neurons in the SNc of AAV5-injected mice (Fig. 1c), we observed the appearance of swollen and distorted h-α-syn+ axons from week 4 onwards, not present in vehicle-injected mice (Fig. 4a and b). Confocal analysis showed increased h-α-syn protein accumulation in the axonal swellings in all brain areas examined (Fig. 4b).

To explore the transport of h-α-syn from SNc/VTA to DA output brain regions such as CPu and, motor M1-2, cingulate and visual V1-2 cortices;[57,58] we examined the co-localisation of h-α-syn^+ and TH^+ axons at 1, 4, 8 and 16 weeks after AAV5 injection into SNc/VTA (Fig. 4a and Supplemental Fig. 3). We found an abundant and progressive presence of h-α-syn^+ axons from 1-week post-injection (Fig. 4c), without significant loss of TH^+ axons in the examined brain

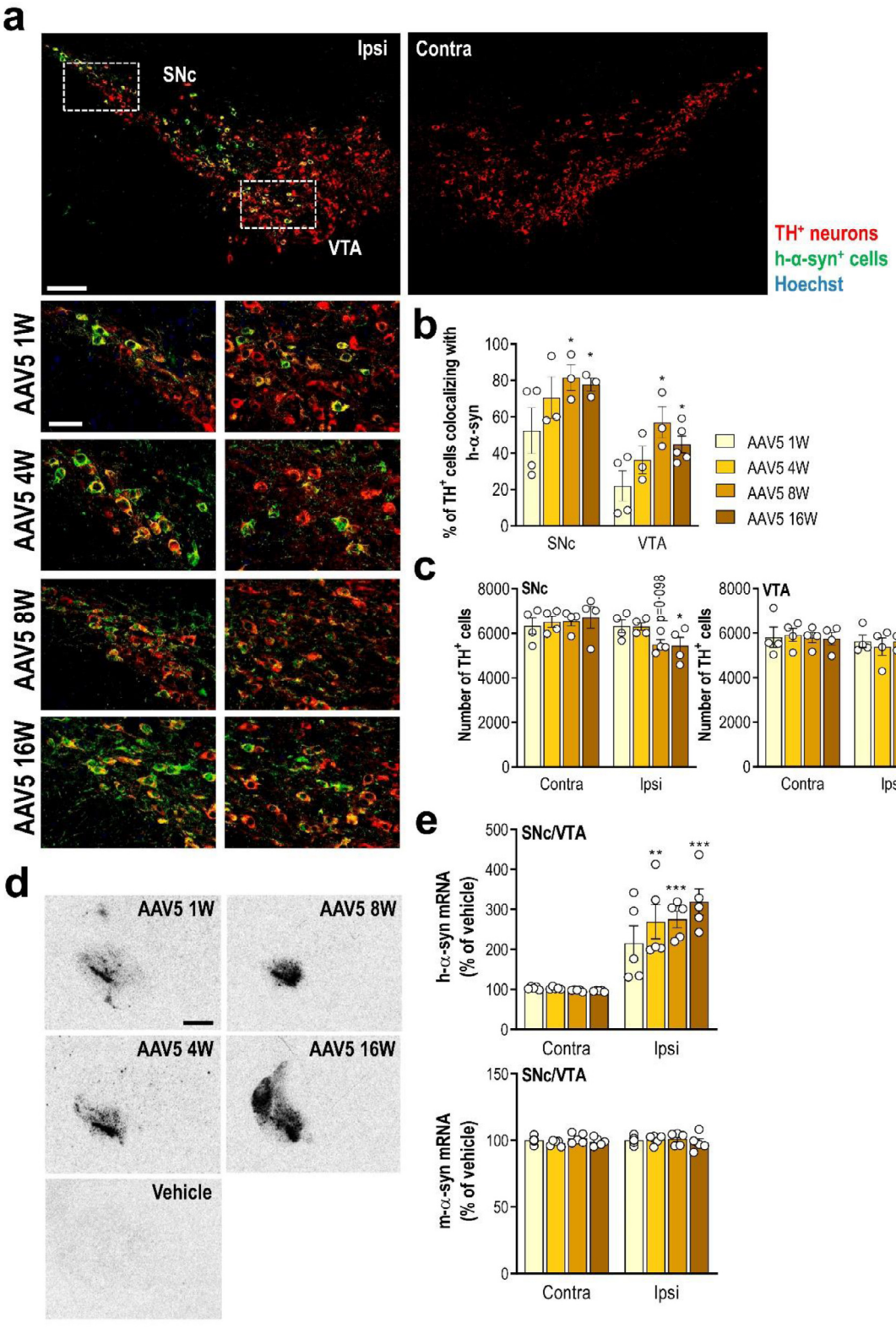

Fig. 1. Overexpression of h-α-syn transgene in SNc/VTA DA neurons of mice. Mice received unilaterally 1 μl AAV5 vector containing a chicken-β-actin promotor to drive expression of wild-type h-α-syn or vehicle into SNc/VTA and sacrificed at 1, 4, 8 and 16 weeks (W) post-injection. (a) Representative confocal images showing the co-localisation of h-α-syn protein and TH$^+$ neurons in ipsilateral (ipsi) SNc/VTA of mice at different time points after AAV5 injection. Scale bar: low = 200 μm, high = 50 μm. (b) Time course showing the number of TH$^+$ cells co-localised with h-α-syn protein in the SNc/VTA of AAV5-injected mice (n = 3–5 mice/group; $^*P < 0.05$ versus 1 W post-injection; two-way ANOVA and Tukey's multiple comparisons test). (c) Number of TH$^+$ cells in ipsi and contralateral (contra) SNc/VTA (n = 4 mice/group; $^*P < 0.05$ versus contra SNc; two-way ANOVA and Tukey's multiple comparisons test). (d) Coronal brain sections showing progressive increases of h-α-syn mRNA levels in the SNc/VTA assessed by *in situ* hybridisation. Scale bar: 1 mm. (e) Increased h-α-syn mRNA expression in the injected side of overexpressed mice compared with vehicle-treated mice. Conversely, no differences were detected for m-α-syn RNA expression in SNc/VTA. See also Supplementary Fig. 2 (n = 5 mice/group; $^{**}P < 0.01$, $^{***}P < 0.001$ versus vehicle-treated mice; two-way ANOVA and Tukey's multiple comparisons test). For all figures, data are represented as mean ± SEM.

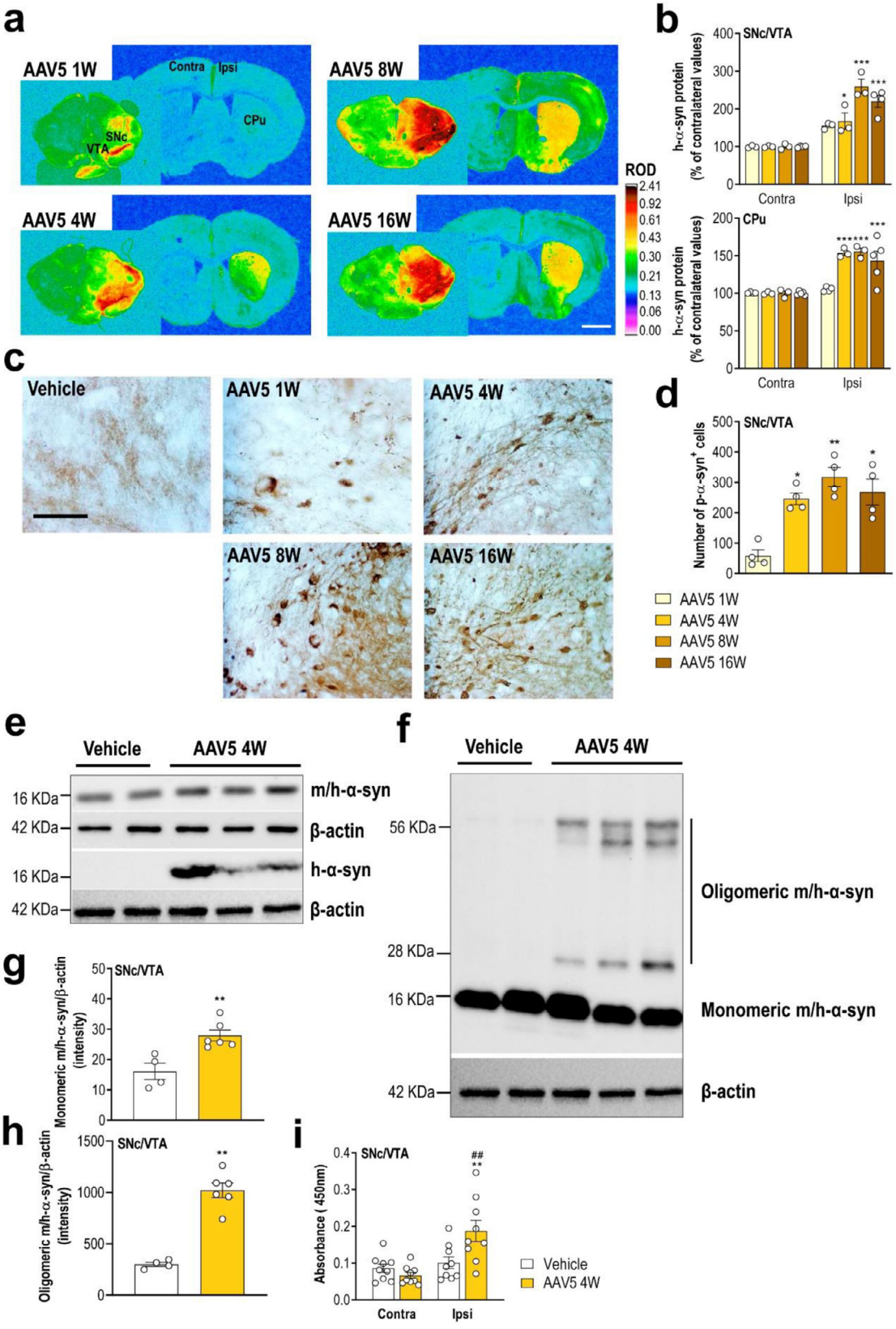

Fig. 2. Progressive accumulation of reactive forms of h-α-syn protein in SNc/VTA. (a) Coronal brain sections showing progressive increases of h-α-syn protein levels in SNc/VTA and CPu assessed by immunohistochemistry procedures. Signal represents the relative optical density (ROD) of autoradiograms. Scale bar: 1 mm. (b) Increased h-α-syn protein levels in the ipsilateral (ipsi) SNc/VTA and CPu versus contralateral (contra) side (n = 3–5 mice/group; $^{*}P < 0.05$, $^{***}P < 0.001$; two-way ANOVA and Tukey's multiple comparisons test). (c) Representative photomicrographs showing gradual increases of phospho-ser129-α-syn protein levels in the SNc/VTA of vehicle- and AAV5-injected mice. Scale bar: 250 μm. (d) Number of phospho-S129-α-syn^{+} cells in the SNc/VTA (n = 4 mice/group; $^{*}P < 0.05$, $^{**}P < 0.01$ versus AAV5-injected mice and sacrificed at 1 week (W) post-infection; one-way ANOVA and Tukey's multiple comparisons test). (e, g) Images of Western blot (e) and quantitative analysis (g) of monomeric α-syn protein in SNc/VTA lysates from mice injected with vehicle or AAV5 (4 W time point). For detection, immunoblots for α-syn were performed using different antibodies against: mouse and human α-syn, and specific human α-syn. β-actin used as loading control (n = 4–6 mice/group; $^{**}P < 0.01$ versus vehicle-injected mice; two-tailed unpaired t-test). (f, h) Immunoblotting (f) and quantification (h) of

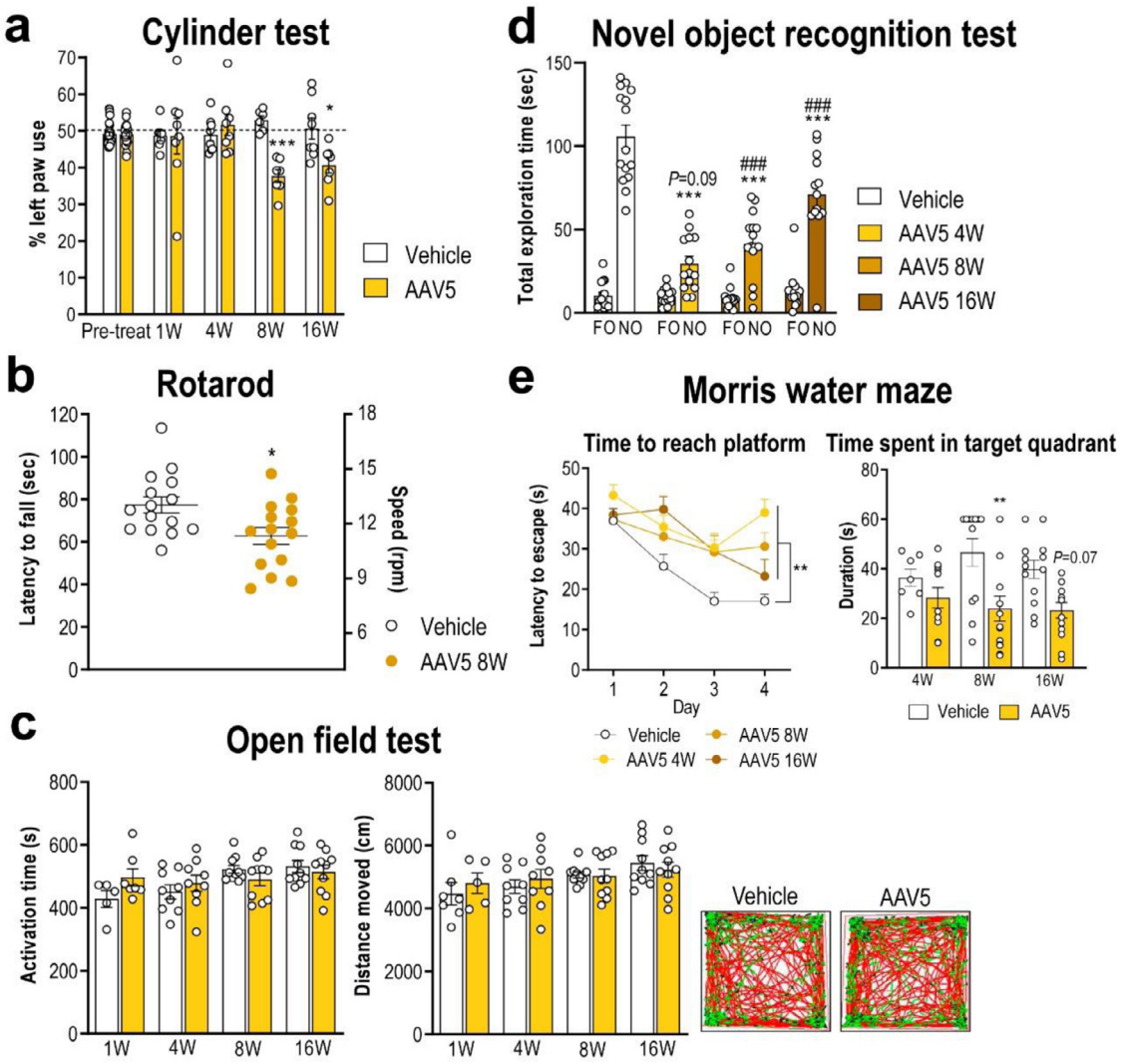

Fig 3. Human-α-syn overexpression in SNc/VTA impairs motor and cognitive behaviours. (a) Mice overexpressing h-α-syn evoked progressive motor deficits in the cylinder test, performing a lesser use of the left paw compared to vehicle-injected mice (n = 10–15 mice/group; $^{*}P < 0.05$, $^{***}P < 0.001$; two-way ANOVA and Sidak's multiple comparison test). (b) At 8 weeks (W) after AAV5 injection, mice also showed alterations in motor coordination in the rotarod, evaluated by a reduction in fall latency and a lower maximum supported speed compared to vehicle-injected mice (n = 15 mice/group; $^{*}P < 0.05$; two-tailed unpaired t-test). (c) Both phenotypes showed a comparable motor activity in the open field test. Representative locomotor activity tracking is showed in the right-hand (n = 5–10 mice/group). (d) Mice overexpressing h-α-syn failed to discriminate between familiar and novel objects (FO and NO, respectively) compared to vehicle-injected mice at different times examined (n = 13–15 mice/group; $^{***}P < 0.001$ versus vehicle-injected mice; $^{\#\#\#}P < 0.001$ versus FO; two-way ANOVA and Sidak's multiple comparison test). (e) In Morris water maze, mice overexpressing h-α-syn showed greater latencies to reach the platform than vehicle-injected mice. Likewise, AAV5-injected mice showed no preference for the target quadrant relative to other quadrants compared to vehicle group (n = 7–13 mice/group; $^{**}P < 0.01$; two-way ANOVA and Sidak's multiple comparison test). See also Supplementary Fig. 2.

areas (Fig. 4d). The highest density of axons co-localising h-α-syn and TH proteins was seen between 8-16 weeks post-injection reaching values of 52.2 ± 5.3%, 42.8 ± 6.1%, 24.9 ± 3.2%, and 14.2 ± 0.4 in CPu > cingulate > motor > visual, respectively. Interestingly, we also detected few scattered TH^{+} and h-α-syn^{+} fibers in the contralateral CPu of AAV5-injected mice at 8 and 16 weeks later, confirming previous anatomical studies showing that approximately 1–3% of the DA fibres reaching the striatum come from the contralateral SNc (Fig. 4a).[59] Moreover, h-α-syn signal was solely axonal and no h-α-syn^{+} cell bodies in DA projection brain areas were detected (Supplemental Fig. 4).

3.4. Reduced striatal and cortical DA neurotransmission in mice overexpressing h-α-syn in SNc/VTA

To confirm whether the accumulation of h-α-syn in forebrain TH^{+} fibres alters DA neurotransmission, we performed microdialysis experiments in CPu and mPFC –containing cingulate, prelimbic and infralimbic subdivisions– of freely moving mice at 4 weeks post-injection. No differences in baseline DA concentration were found in both CPu and mPFC between the different groups (Table 1). However, local veratridine infusion (50 μM, depolarizing agent) by reverse dialysis increased extracellular DA levels in CPu and mPFC of vehicle-

α-syn oligomer sum in SNc/VTA lysates from the same mice using anti-α-syn antibody against mouse and human, and anti-β-actin antibody as loading control (n = 4–6 mice/group; $^{**}P < 0.01$ versus vehicle-injected mice; two-tailed unpaired t-test). (i) Increased oligomer α-syn levels in SNc/VTA lysates of vehicle- and AAV5-injected mice at 4 W post-injection assessed by ELISA using anti-α-syn filament antibody (n = 9 mice/group; $^{**}P < 0.01$ versus vehicle-injected mice, $^{\#\#}P < 0.01$ versus contralateral -contra- side; two-way ANOVA and Tukey's multiple comparisons test).

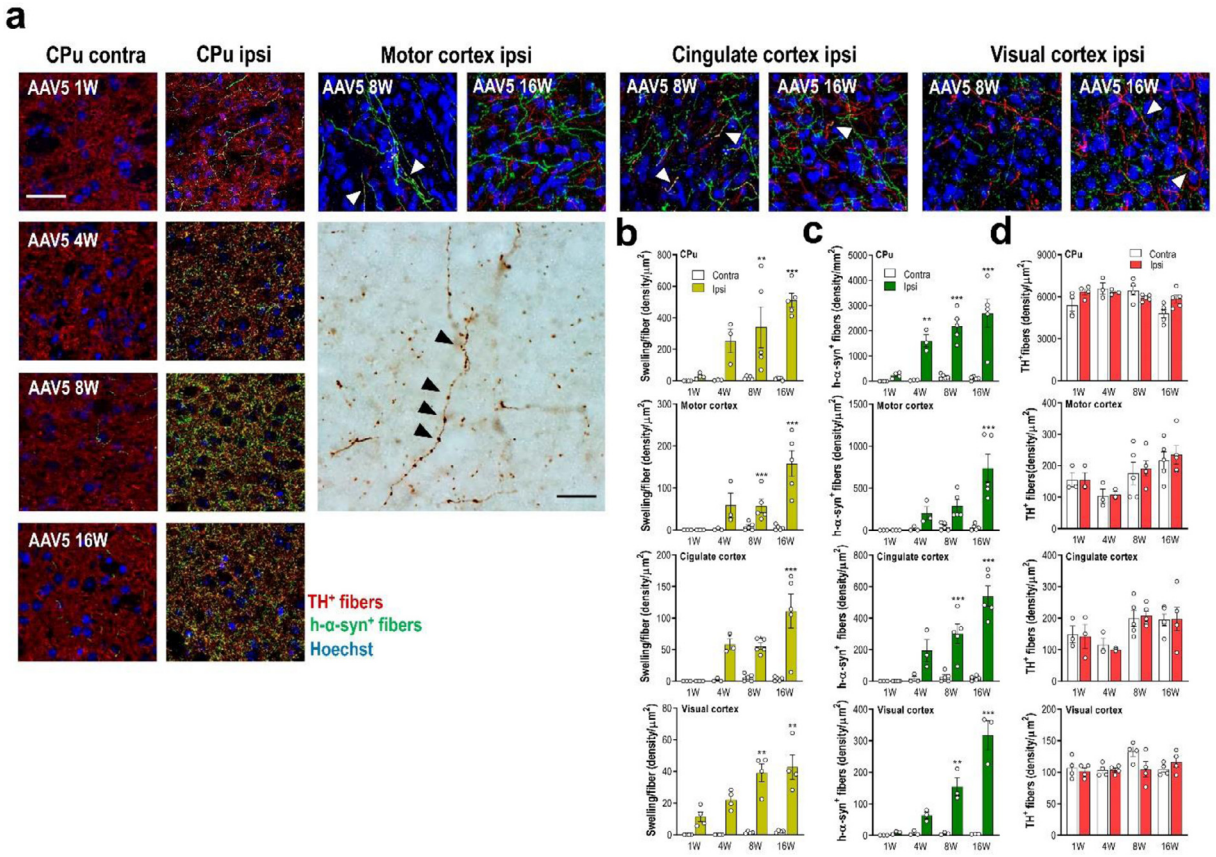

Fig. 4. Human-α-syn overexpression in DA neurons induces axonal pathology in connected brain regions. (a) Representative confocal images showing h-α-syn protein co-localised with TH$^+$ fibres in DA output brain regions such as CPu, and motor, cingulate and visual cortices of AAV5-injected mice examined at 1, 4, 8 and 16 weeks (W) later. TH$^+$ and h-α-syn$^+$ fibres are identified with white arrowheads. Scale bar: 25 μm. Likewise, a representative image shows h-α-syn$^+$ axonal swellings in motor cortex assessed by immunohistochemistry procedure. Axonal swellings are identified with black arrowheads. Scale bar: 100 μm. (b) Progressive accumulation of h-α-syn$^+$ axonal swelling density in the different brain areas examined. (c) Progressive increases of h-α-syn$^+$ fibre density in the different brain area examined. (d) Density of TH$^+$ fibres in different DA innervated brain regions of mice. Overexpression of h-α-syn in SNc/VTA did not induce loss of DA terminals at 1, 4, 8 and 16 W post-infection (n = 3–5 mice/group; $^*P < 0.05$, $^{**}P < 0.01$, $^{***}P < 0.001$ versus to AAV5-injected mice and sacrificed 1 W later; two-way ANOVA and Tukey's multiple comparisons test). See also Supplementary Figs. 3 and 4.

treated mice to a larger extend than in mice overexpressing h-α-syn (Fig. 5a, b and Supplemental Fig. 5).

We have previously shown that *in vivo* DAT function in DA terminals is regulated by α-syn.[31] The infusion of DAT inhibitor, nomifensine (1-10-50−μM), dose-dependently increased extracellular DA concentration in CPu and mPFC. This effect was more pronounced in the control group than in mice overexpressing h-α-syn. Likewise, local infusion of amphetamine (1-10-100 μM) significantly increased DA release in CPu and mPFC, an effect which was greater in vehicle-injected mice than in AAV5-injected mice (Fig. 5c–f). Moreover, we also examined the effect of DA D2 receptor agonist quinpirole (10 μM) on DA release. While quinpirole infusion in mPFC decreased DA release similarly in both phenotypes, the reduction of quinpirole-induced striatal DA release was only found in vehicle-injected mice, but not in AAV5-injected mice, suggesting that the inhibitory feedback mechanism mediated by DA D2 receptor activation is markedly attenuated after h-α-syn overexpression (Fig. 5g and h). These results are consisted with earlier findings suggesting that increased α-syn expression reduces neurotransmitter release.[31,60]

Table 1
Baseline DA dialysate concentrations in the CPu and mPFC of mice

		DA	
Groups	Experimental Conditions	CPu	mPFC
Vehicle	aCSF + DMSO (a)	11.7 ± 0.9 (9)	8.4 ± 1.0 (6)
AAV5	aCSF + DMSO (a)	11.9 ± 0.7 (7)	9.6 ± 0.7 (5)
Vehicle	aCSF (a)	10.1 ± 0.8 (13)	6.25 ± 0.8 (9)
AAV5	aCSF (a)	13.7 ± 2.2 (12)	5.02 ± 0.3 (10)
Vehicle	aCSF + Nom (a)	29.0 ± 5.6 (4)	9.3 ± 1.8 (4)
AAV5	aCSF + Nom (a)	21.3 ± 5.1 (5)	7.2 ± 0.7 (5)
AAV5 + Vehicle	aCSF + DMSO (b)	10.1 ± 0.8 (5)	n.e
AAV5 + IND-1337-ASO	aCSF + DMSO (b)	11.2 ± 0.9 (5)	n.e
AAV5 + Vehicle	aCSF (b)	12.2 ± 1.6 (10)	n.e
AAV5 + IND-1337-ASO	aCSF (b)	14.8 ± 1.4 (10)	n.e
Vehicle	aCSF + Nom (b)	25.8 ± 4.9 (6)	n.e
AAV5	aCSF + Nom (b)	28.3 ± 4.4 (6)	n.e

Extracellular DA levels are expressed as fmol/20 min fraction. In the experiments involving the evaluation of veratridine and quinpirole effects on extracellular DA levels, dimethyl-sulfoxide (DMSO) or nomifensine (Nom) 10 μM were added in the artificial cerebrospinal fluid (aCSF), respectively. Data are means ± SEM of the number of mice shown in parentheses. (a) Dialysis probe was preparing using the Cuprophan membrane, 6000 Da molecular weight cut-off. (b) Dialysis probes were provided from CMA (ref.; CMAP000083). n.e. not examined.

3.5. ASO therapy prevents h-α-syn accumulation and alleviates DA neurotransmission deficits in the PD-like mouse model

Recently, we reported that an indatraline-conjugated ASO (IND-1233-ASO) selectively reduced murine α-syn expression in monoaminergic neurons of wild-type mice.[31] This specificity is due to the potent *in vitro* affinity and *in vivo* occupancy of indatraline for monoamine transporters,[61] which allows the accumulation of oligonucleotide in this neuronal population after intranasal administration. Here, we extended this previous study and designed a specific ASO

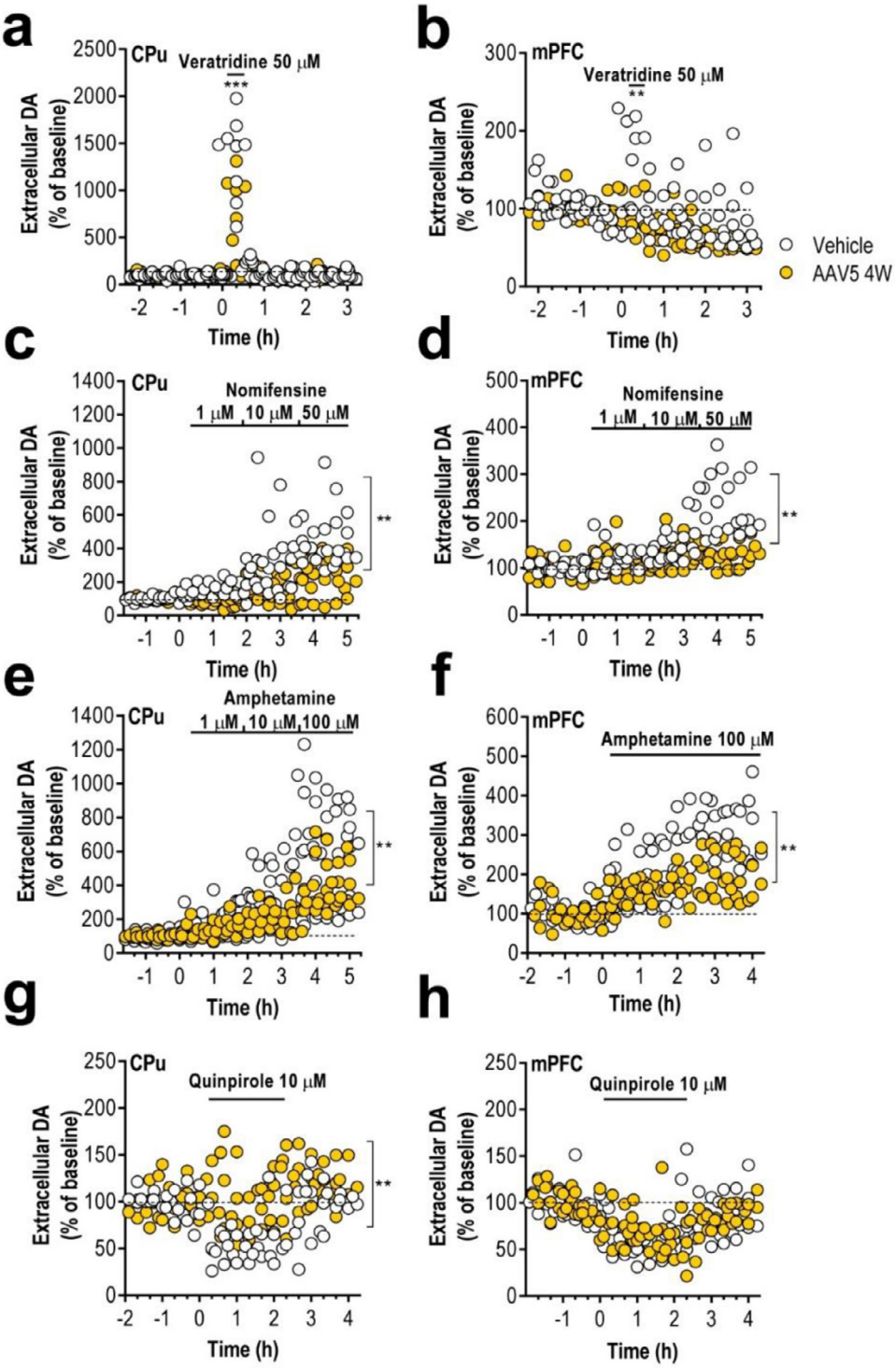

Fig. 5. Human-α-syn overexpression in SNc/VTA induces reduced DA neurotransmission in forebrain. (a–b) Local veratridine infusion (depolarizing agent; 50 μM) significantly increased DA release in CPu (a) and mPFC (b) of both phenotypes of mice. However, this effect was significant less in AAV5-injected than in vehicle-injected mice. (c–d) Local application of nomifensine (DAT inhibitor; 1, 10 and 50 μM) increased dose-dependently extracellular DA concentration in CPu (c) and mPFC (d), being this effect greater in vehicle-injected than in AAV5-injected mice. (e–f) Similarly, direct infusion of amphetamine (DA releaser and DAT inhibitor; 1, 10 and 100 μM) by reverse dialysis induced increases of DA release in both CPu (e) and mPFC (f), being the effect significantly more pronounced in vehicle-injected compared to AAV5-injected mice. (g–h) Local activation of DA D2 receptors with quinpirole (DA D2 agonist, 10 μM) decreased the striatal DA release (g) in vehicle-injected mice, but not in mice overexpressing h-α-syn. However, local quinpirole infusion produced similar effects on DA release in mPFC (h) of both phenotypes (n = 5–10 mice/group; $^{*}P < 0.05$, $^{**}P < 0.01$, $^{***}p < 0.001$ compared to vehicle-injected mice; two-way ANOVA and Tukey's multiple comparisons test). Data were recorded as repeated measures with each individual replicate. See also Supplementary Fig. 5.

sequence targeting h-α-syn in the AAV5-induced α-overexpression model that was conjugated with indatraline (IND-1337-ASO) and applied intracerebroventricular or intranasally (Fig. 6a and 7a). Mice injected with AAV5 into SNc/VTA were treated intracerebroventricularly with either vehicle or nonsense IND-1227-ASO (100 μg/day) or IND-1337-ASO (30 or 100 μg/day) for 28 days and euthanized at different times after completion of treatment (Fig. 6a). The IND-1337-ASO administration significantly reduced h-α-syn transgene expression compared to AAV5-injected mice and treated with either vehicle or IND-1227-ASO (Fig. 6b and c). The reduction of h-α-syn mRNA

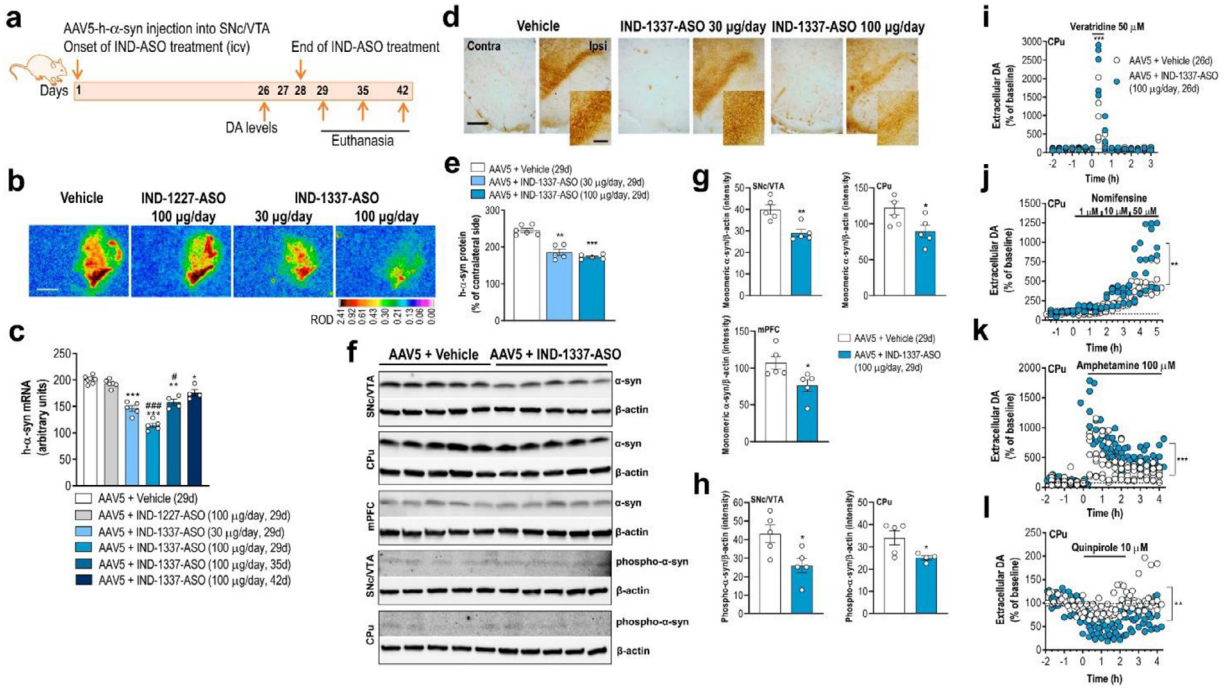

Fig. 6. Intracerebroventricular conjugated ASO therapy prevents h-α-syn accumulation and recovers DA neurotransmission deficits. (a) Treatment timeline. Mice were unilaterally injected with 1 μl AAV5 into SNc/VTA and also received: i) vehicle, ii) IND-1227-ASO (100 μg/day) or iii) IND-1337-ASO (30 or 100 μg/day) into the lateral ventricle for 28 days using osmotic minipumps. Mice were sacrificed at 24 h, 1 week or 2 weeks later (days 29, 35 and 42, respectively). (b) Coronal brain sections showing h-α-syn mRNA expression in SNc/VTA of AAV5-injected mice and treated with vehicle, IND-1227-ASO or IND-1337-ASO assessed by *in situ* hybridisation procedures. Scale bar: 1 mm. Signal represents the relative optical density (ROD) of autoradiograms. See also Supplementary Fig. 6. (c) Decreased h-α-syn mRNA expression in AAV5-injected mice treated with IND-1337-ASO compared to control groups. Reduction of h-α-syn production was dose- and time-dependent, leaving a significant decreased transgene expression up to 14 days after treatment (day 42) (n = 4–7 mice/group; $^{*}P < 0.05$, $^{**}P < 0.01$, $^{***}P < 0.001$ versus AAV5 + vehicle group; $^{\#}P < 0.05$, $^{\#\#\#}P < 0.001$ versus AAV5 + IND-1227-ASO group; one-way ANOVA and Tukey's multiple comparisons test or unpaired t-test). (d) Coronal brain sections showing h-α-syn protein levels in SNc/VTA of mice assessed by immunohistochemistry procedures in frozen tissue. Scale bar: low = 200 μm and high = 50 μm. (e) Human-α-syn protein levels were dose-dependently reduced in AAV5-injected mice and treated with IND-1337-ASO compared to AAV5 + vehicle group (n = 5–6 mice/group; $^{**}P < 0.01$, $^{***}P < 0.001$; one-way ANOVA and Tukey's multiple comparisons test or unpaired t-test). (f–h) Immunoblotting (f) and quantification of monomeric α-syn (g, 16 KDa) and phospho-ser129-α-syn (h, 16 KDa) in SNc/VTA, CPu and mPFC lysates from the same AAV5 mice treated with vehicle or IND-1337-ASO (100 μg/day). β-actin used as loading control (n = 5 mice/group; $^{*}P < 0.05$, $^{**}P < 0.01$ versus AAV5 + vehicle group; unpaired t-test). (i–l) Microdialysis approach using different dopaminergic agents as in Fig. 5 confirmed an improvement of DA neurotransmission in the CPu of AAV5 mice treated with IND-1337-ASO (100 μg/day) compared to vehicle-treated mice (n = 4–6 mice/group; $^{**}P < 0.01$, $^{***}P < 0.001$; two-way ANOVA and Tukey's multiple comparisons test).

levels was dose- and time-dependent, reaching a maximum decrease 1 day after finalisation of treatment –day 29– (AAV5 + vehicle: 200 ± 2; AAV5 + IND-1337-ASO 30 μg/day: 146 ± 5; AAV5 + IND-1337-ASO 100 μg/day: 114 ± 4, arbitrary units). Nevertheless, intracerebroventricular IND-1337-ASO therapy (100 μg/day) elicited significant reductions of transgene expression until 14 days post-treatment –day 42– (Fig. 6c). Likewise, intranasal IND-1337-ASO administration (100 μg/day, 28 days) also reduced h-α-syn mRNA expression in SNc/VTA, although this effect size was less than after intracerebroventricular application (Fig. 7b and c). Remarkably, IND-1337-ASO treatment did not induce any change in TH and DAT mRNA levels neither in SNc/VTA nor in murine α-syn expression, which supports the specificity and safety of ASO sequence (Supplemental Fig. 6). The reduced expression of SNc/VTA h-α-syn mRNA levels was accompanied by a significant decrease of h-α-syn protein as assessed by immunohistochemistry (Fig. 6d, e, 7d and e) and Western blot analysis (Fig. 6f and g). Furthermore, α-syn protein accumulation also decreased in connected DA brain areas, such as CPu and mPFC (Fig. 6f and g). In parallel, a reduction in the toxic phospho-S129-α-syn levels was detected in SNc and CPu from mice injected with AAV5 and treated with IND-1337-ASO compared to AAV5 mice treated with vehicle (Fig. 6f and h).

Next, we found that AAV5-injected mice and treated with IND-1337-ASO (100 μg/day, intracerebroventricular) showed an improved DA neurotransmission in the nigrostriatal pathway (Fig. 6i–l). Local veratridine infusion (50 μM) significantly increased striatal DA release in mice overexpressing h-α-syn and treated with IND-1337-ASO compared to mice receiving vehicle (Fig. 6i). In addition, local nomifensine infusion (1-10-50 μM) increased dose-dependently extracellular DA concentration in CPu. This effect was more pronounced in IND-1337-ASO-treated than in vehicle-treated mice (Fig. 6j). Likewise, amphetamine application (100 μM) also increased extracellular DA levels in CPu being greater in AAV5 mice treated with IND-1337-ASO than with vehicle (Fig. 6k). Finally, IND-1337-ASO treatment restored DA D2 receptor-induced inhibitory feedback mechanism controlling striatal DA release as assessed by local quinpirole infusion (Fig. 6l). Overall, these data indicate that the reversible reduction of h-α-syn synthesis and accumulation by IND-1337-ASO is able to prevent early deficits of DA neurotransmission in the PD-like mouse model, even when behavioural alterations are not evident and appear at a later stage.

3.6. Reduced α-Syn protein levels in monoaminergic brain areas of nonhuman primates after ASO treatment

Next, we examined the selectivity of the brain delivery of IND-conjugated ASO in rhesus macaques, whose brain anatomy is closer to the human brain. The designed IND-1233-ASO sequence, completely complementary to murine, nonhuman primate and human α-syn mRNA,[31] was infused at a dose of 1 mg/day in the right lateral ventricle for 28 days (Fig. 8a). The IND-1233-ASO dose was chosen based on previous studies using potential therapeutic ASOs in macaque models of amyotrophic lateral sclerosis (1 mg/day, intracerebroventricular, for 14 days) or Huntington's disease (4 mg/day, intrathecal administration for 21 days).[62,63] Furthermore, the appropriate dose used herein for nonhuman primates was also based on

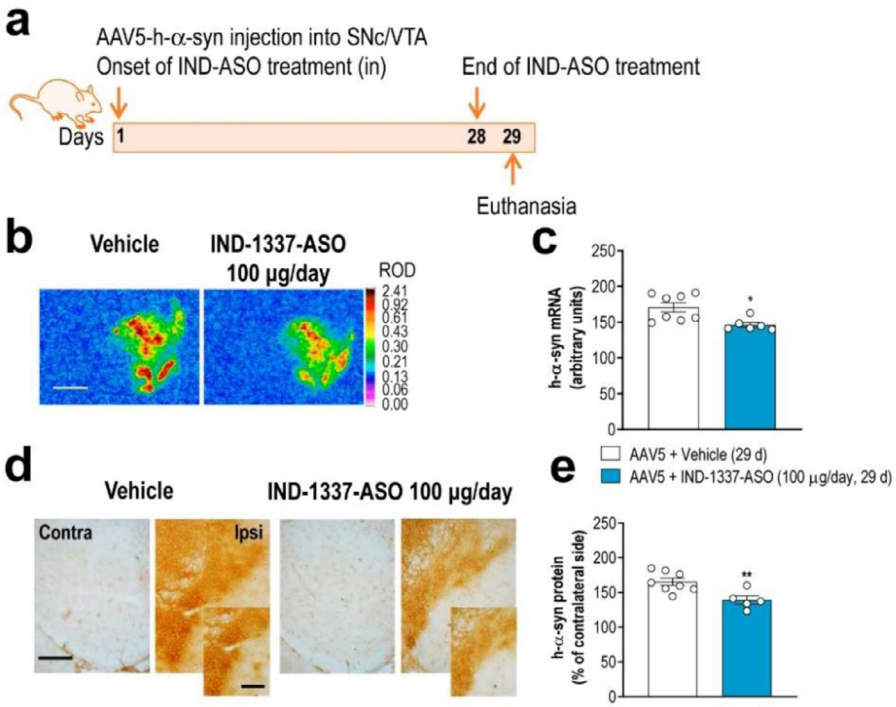

Fig. 7. Intranasal treatment with conjugated ASO prevents AAV5-mediated h-α-syn production. (a) Treatment timeline. Mice were unilaterally injected with 1 μl AAV5 into SNc/VTA and intranasally administered with: i) vehicle or ii) IND-1337-ASO (100 μg/day) for 28 days. Mice were sacrificed 24 h later at 29 days. (b) Coronal brain sections showing h-α-syn mRNA expression in SNc/VTA of AAV5-injected mice and treated with vehicle or IND-1337-ASO assessed by *in situ* hybridisation procedures. Scale bar: 1 mm. Signal represents the relative optical density (ROD) of autoradiograms. (c) Decreased h-α-syn mRNA expression in AAV5-injected mice treated with IND-1337-ASO compared to control group (n = 6–8 mice/group; $^{*}P < 0.05$; unpaired t-test). (d) Coronal brain sections showing h-α-syn protein levels in SNc/VTA of the same mice assessed by immunohistochemistry procedures in frozen tissue. Scale bar: low = 200 μm and high = 50 μm. (e) Reduction of h-α-syn protein level in AAV5-injected mice treated with IND-1337-ASO (n = 6–8 mice/group; $^{**}P < 0.01$; unpaired t-test).

the IND-1233-ASO toxic-kinetic profile evaluated in mice (see Supplemental information on mouse toxicity studies). Hence, IND-1233-ASO was well tolerated during the 4 weeks of treatment and, no changes were found in daily observed behavioral variables, such as drinking, eating and body temperature in rhesus macaques compared to vehicle-treated monkeys.

At 1 day after the end of infusion, α-syn protein levels in the SN medial of IND-1233-ASO-infused animals were significantly reduced to 48% and 40% of the control levels, as assessed by Western blot assay and ELISA, respectively (Fig. 8b and c). Likewise, we found reductions of α-syn protein levels in other monoaminergic brain regions such as the VTA and dorsal raphe nucleus, although statistical analysis showed a marginal effect of group (P = 0.059 and P = 0.096, respectively). The decrease in α-syn protein levels in the midbrain monoaminergic regions was parallel to the accumulation of complete oligonucleotide in these brain areas, unlike cerebrospinal fluid, where fragments of the degraded molecule were detected (unpublished observation). However, α-syn protein density did not change in anatomically connected monoaminergic networks (i.e., globus pallidus, putamen, frontal cortex, motor cortex and cerebellum) of monkeys treated with IND-1233-ASO compared to monkeys treated with vehicle, as previously found in AAV5 PD-like mouse model. Overall, these data indicate that a longer duration/dosing of IND-1233-ASO treatment may be required to suppress α-syn protein accumulation through the monoaminergic connectome.

4. Discussion

Here, we present novel data showing the benefit of a sustained conjugated ASO therapy to reduce α-syn synthesis in vulnerable monoamine-rich brain areas, as assessed in a mouse model overexpressing h-α-syn in SNc/VTA and in aged nonhuman primates. Interestingly, conjugated ASO therapy also decreased α-syn protein accumulation and its phosphorylated monomeric form through the dopaminergic connectome, and prevented the deficits in forebrain DA neurotransmission in the PD-like mouse model. While IND-1337-ASO was designed specifically to target h-α-syn transgene cloned in the AAV5 vector, IND-1233-ASO was designed such that the target mRNA sequence displays homology to murine, rhesus macaque and human α-syn. Remarkably, the absence of DA neuronal toxicity induced by the IND-1233-ASO previously reported in wild-type mice,[31] and the selectivity thereof to reduce the α-syn protein in DA neurons of mice and nonhuman primates warrants further research to assess the benefit of oligonucleotide-based non-viral gene therapy as a disease modifying therapy for PD and related synucleinopathies.

As a methodological consideration about the AAV5 viral vector expressing wild-type h-α-syn used herein, we should mention that it was previously validated *in vivo* in rats as reported at the Michael J. Fox Foundation's research tools website (https://www.michaeljfox.org/research-tools-catalog).[39] Here, we show for the first time that mice successfully expressed the transgene using the same AAV5 construct, and exhibited cellular and functional deficits characteristic of the early stages of PD, with a modest DA neuronal loss in SNc. Together, this suggests the utility and reproducibility of this tool in rodent species to test the prospective therapeutics targeting α-syn.

A selective reduction of α-syn production was found in midbrain monoaminergic regions of mice and nonhuman primates by exploiting our previous strategy, in which different oligonucleotides were covalently bound to monoamine transporter inhibitors for the selective delivery of them to monoaminergic cells *in vivo*.[29–32] While indatraline-conjugated ASO enters directly in the cerebrospinal fluid circulation after intracerebroventricular infusion, the precise mechanism(s) by which indatraline-conjugated ASO reaches monoamine neuronal groups after intranasal administration are not fully clarified. Recent observations suggest that this mechanism involved (i) an extracellular diffusion into the olfactory submucosa along open

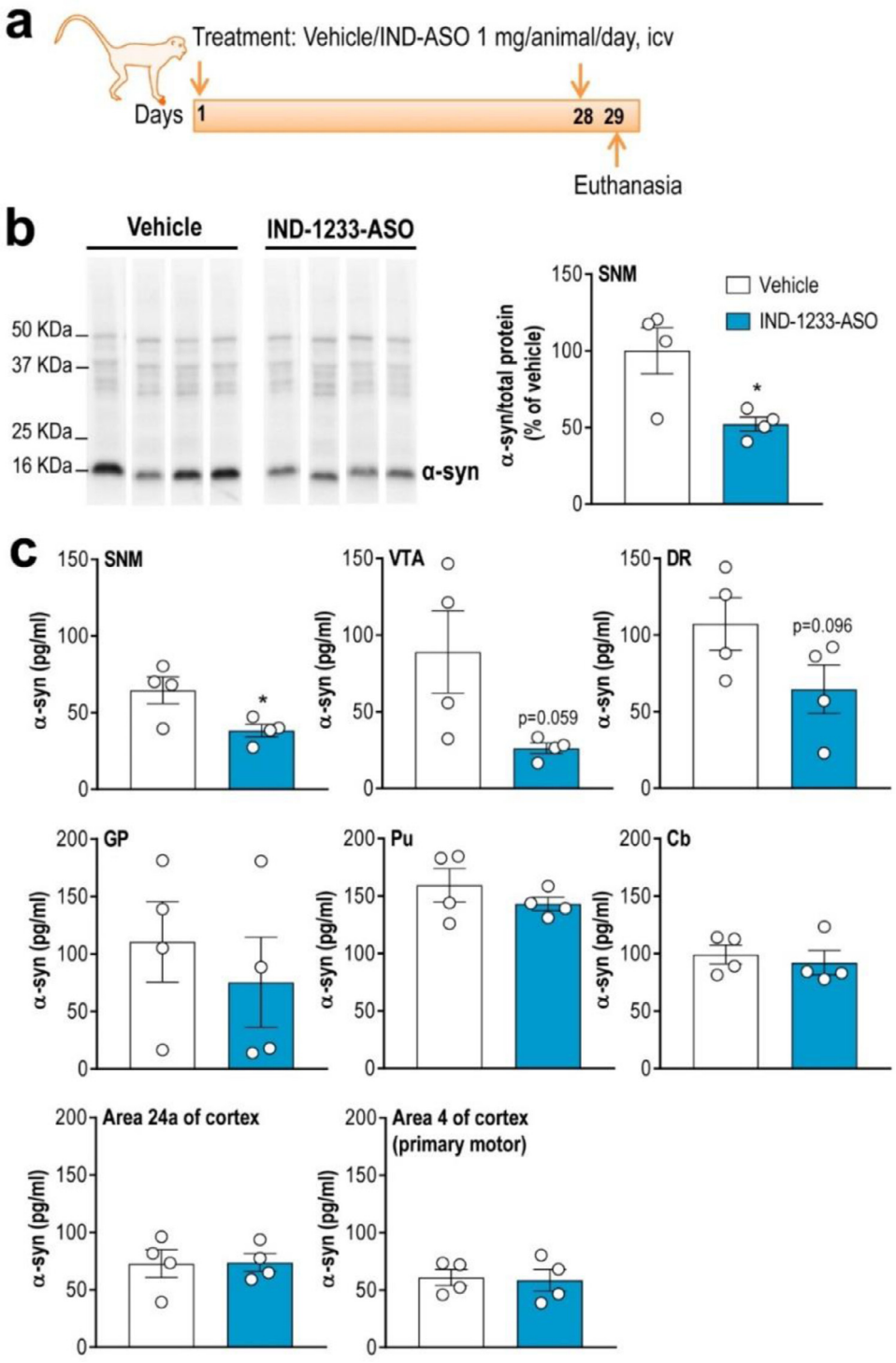

Fig. 8. Conjugated ASO therapy decreases α-syn protein levels in midbrain monoaminergic areas of nonhuman primates. (a) Treatment timeline. Elderly rhesus monkeys received vehicle or IND-1233-ASO (1 mg/day) into the right lateral ventricle for 28 days using osmotic minipumps and sacrificed at 24 h later. (b) Western blot images of α-syn protein levels in substantia nigra medial (SNM) of vehicle- and IND-1233-ASO-tretated nonhuman primates. Coomassie-stained gels were used as loading control showing equal loading at top. Bar graphs showing a significant decrease of α-syn protein levels in SNM compared to vehicle-treated rhesus macaques. (c) A significant reduction of α-syn protein levels in SNM, and marginal effects on α-syn protein synthesis in VTA and dorsal raphe nucleus (DR) of monkeys treated with IND-1233-ASO were found compared to vehicle-treated monkeys assessed by ELISA. No differences were achieved in projection brain areas including globus pallidus (GP), putamen (Pu), frontal and motor cortices (areas 24a and 4, respectively), and cerebellum (Cb) (n = 4 monkeys/group; $^*P < 0.05$ compared to vehicle-nonhuman primates; unpaired t-test).

intercellular clefts, (ii) a rapid transport into the olfactory subarachnoid space and entry into the cerebrospinal fluid circulation and, (iii) uptake of indatraline-conjugated ASO by the dense network of axons emerging from monoamine cell bodies, which contain the highest densities of SERT, DAT, and NET of all brain.[31,64,65] Probably, this is also the mechanism by which IND-1337-ASO reaches DA neurons in the AAV5 mouse model after intranasal administration, since the enrichment of conjugated oligonucleotides in monoamine neurons does not depend on the oligonucleotide sequence as previously reported.[29,30]

In wild-type mice, short term intranasal treatment with IND-1233-ASO (30 μg/mouse/day, 4 days) produced a sustained reduction

of endogenous α-syn expression in monoamine neurons up to 7 days post-administration, which resulted in an enhanced DA and 5-HT neurotransmission.[31] In the present study, both intracerebroventricular and intranasal treatments with IND-1337-ASO (100 μg/mouse/day, 28 days) prevented h-α-syn mRNA and protein accumulation in the SNc/VTA of AAV5 mouse model, without affecting endogenous α-syn level. Importantly, the 30−40% decrease of h-α-syn mRNA levels obtained after intracerebroventricular treatment (~20% reduction after intranasal administration) did not induce DA neurotoxicity as assessed by TH and DAT mRNA expression. Remarkably, and of high relevance for the design of ASO-based therapies, the reduction of h-α-syn expression persists for 14 days after intracerebroventricular IND-1337-ASO administration, when h-α-syn mRNA levels returned to its initial level. Nevertheless, using shRNA cloned in AAV vector to knockdown α-syn (>70% of decrease), some reports indicated degeneration of DA neurons and striatal denervation in rats and nonhuman primates.[24−27] These data are important in the context of ongoing attempts to develop PD therapeutics targeting α-syn expression. Since PD is a chronic disease, it is likely that prolonged therapeutic knockdown of α-syn expression would be required to stop pathogenesis and disease progression. Uses of viral vectors −essentially retroviruses, lentiviruses and AAV− have thus far eclipsed uses of non-viral vectors for gene therapy delivery in the clinic. Viral vectors have certain issues involving genome integration, the inability to be delivered repeatedly, and possible host rejection. Fortunately, alternatives to viral strategies are currently being developed based on non-viral oligonucleotides (siRNA, ASO, miRNA mimics).[66−69] Non-viral approaches are biologically safer and much less immunogenic that viral vectors.[70,71] Conversely, for non-viral oligonucleotides to be effective, they must achieve delivery to affected regions or cells at appropriate concentrations. Furthermore, they must be stable, therefore they require additional protection measures (end-blocking, base modification, etc.), and maintain efficacy over time for feasible treatment throughout the course of disease.[72] Brain diseases often pose problems that limit efficient and effective drug delivery, and once in the brain compartment, another limitation is delivery to selected neuronal populations. To overcome these challenges, strategies are being implemented including the use of nanoparticles to protect oligonucleotides from endonuclease degradation by increasing their stability, as well as covalent conjugation of oligonucleotides with small molecules to target selective brain cells, as reported here. It is unclear at this stage which viral *versus* non-viral gene therapy modality will prove safest, most effective, and practicable in the clinical setting. Non-viral oligonucleotides are constantly being modified and restructured to enhance their target potency and improve delivery. In particular, ASOs are emerging as a potential therapeutic strategy to reduce α-syn production in PD given their specificity, flexibility and overall safety.

Previous studies showed that AAV-mediated overexpression of h-α-syn in rodent SNc/VTA replicates many of the neuropathological features of human disease, including phospho-S129-α-syn pathology and progressive DA cell loss.[73,74] Expression of the transgene depends not only on the AAV serotype and the number of viable vector particles injected, but also on the efficiency of gene expression, which in turn is determined by the vector construct design, and the promoter used (chicken-β-actin, synapsin, etc.).[39,74−78] While our results clearly showed that the AAV5-induced overexpression of h-α-syn in SNc/VTA DA neurons leads a mild neuronal degeneration, DA neurons expressing the transgene had abnormal processes with h-α-syn protein accumulation along the DA connectome, and developed a dystrophic axonal morphology. In parallel, PD-like mice exhibited reduced DA neurotransmission in the nigrostriatal and mesocortical pathways at the beginning of the fourth week post-injection. In addition, mice showed motor and cognitive deficits, especially in the last phase (8 and 16 weeks after AAV5 injection), when h-α-syn and phospho-S129-α-syn protein levels were maximal. These above observations emphasise the fact that the behavioural phenotype of DA deficits is not only a result of cell death, but that functionally impaired surviving neurons contribute to the outcome and should be considered as a target for treatment. Thus, a potential attenuation of α-syn expression/function could contribute to recue deficits in DA neurotransmission since α-syn modulates neuronal DA activity.[31] In fact, IND-1337-ASO treatment (100 μg/mouse/day, 28 days) not only prevented h-α-syn protein accumulation in SNc/VTA and in anatomically connected brain areas, avoiding the disruption of a variety of normal cellular processes, but also enhanced the DA neurotransmission reaching the levels of intact mice. Although we have not examined whether this is sufficient to improve the late-onset behavioural phenotype, we have normalised DA function in the PD-like mouse model.

Finally, in contrast to prior approaches, the present study takes advantage to establish a delivery strategy of conjugated ASO (IND-1233-ASO) effectively achieving a selective reduction of α-syn protein in monoaminergic cell groups such as SN medial and in a lower proportion in VTA and dorsal raphe nucleus of rhesus macaques. Although this pilot study in non-human primates has clear limitations, the present results confirm and extend our previous findings in wild-type mice showing that the same IND-1233-ASO sequence effectively decreased endogenous α-syn protein to 40% in these neuronal groups,[31] showing the high translational value of ASO approach. There is compelling evidence demonstrating that the loss of monoamine neurons -mainly DA neurons, but also norepinephrine and serotonin neurons- is one of the first degenerative events taking place in the brains of PD patients, and that the accumulation and aggregation of α-syn may be a trigger for this early pathological cascade.[9,36,79−82] To date, only two studies have reported that direct infusion of a non-viral siRNA or a viral vector delivering short hairpin RNA targeted endogenous α-syn into SNc of nonhuman primates achieved a 40 to >80% reduction, respectively, of α-syn expression.[18,26] Of importance, the latter study reproduced the pattern of nigrostriatal degeneration characteristics of PD,[26] arguing for the need to maintain a threshold for α-syn knockdown since this protein is essential for neuronal homeostasis and neurotransmission, and its elimination would dramatically impact brain function. While clinical interventions with oligonucleotide therapeutics (ASO, siRNA, miRNA) have a long way to go, numerous recent advances in modified oligonucleotide technology and improvements in delivery systems highlight RNA therapeutics as a cutting-edge treatment for neurodegenerative diseases.[22,66-69] In this regard, several reports suggest that partial suppression of target gene expression is well tolerated in nonhuman primates and further supports oligonucleotides as potential therapy for amyotrophic lateral sclerosis or Huntington's diseases.[69,83]

In conclusion, using mouse and nonhuman models, the present study provides an initial demonstration that a new conjugated therapeutic ASO reduces α-syn synthesis selectively in midbrain monoaminergic regions and their connectome over a sustained period of time and may be enough to alleviate deficiencies in DA neurotransmission and associated α-syn pathology, at least by reducing its phosphorylated monomeric form. Further studies in suitable PD-like models will be needed to assess the efficacy of ASO treatment on the toxic aggregates of phospho-α-syn in its different high molecular weight species. For diseases such as PD, where α-syn protein accumulation is tolerated for decades prior to disease onset, this finding opens the possibility that transient suppression of α-syn mRNA can lead to a prolonged effect in patients. Indeed, this raises the prospect that a decrease in α-syn production in locally vulnerable monoamine neurons may allow the global clearance of reactive α-syn species in anatomically connected regions. This study highlights that the conjugated ASO used offers an early intervention strategy to delay PD progression, something that might be attractive in conjunction with current immunotherapy trials targeting α-syn protein, or those with anti-aggregation agents.

Acknowledgements

We thank M. Calvo and E. Coll for outstanding technical support in the confocal microscopy unit (CCiT-UB). We thank to the Coordenação de Aperfeiçõamento de Nivel Superior (CAPES- PDSE: 19/2016 88881.135527/2016-01), Brazil, for their financial scholarship support to V.C-S. We would also like to thank Prof. Silvio Zanata for his valuable comments of the significance of results.

Funding

This study was supported by grants SAF2016-75797-R, Retos-Colaboración Subprogram RTC-2014-2812-1 and RTC-2015-3309-1, Ministry of Economy and Competitiveness (MINECO) and European Regional Development Fund (ERDF), UE; Therapeutic Pipeline Program Spring 2014 Program, grant ID: 9238, The Michael J. Fox Foundation; Centro de Investigación Biomédica en Red de Salud Mental (CIBERSAM), and Centro de Investigación Biomédica en Red de Enfermedades Neurodegenerativas (CIBERNED).

Competing interests

R. Revilla, A. Montefeltro, F. Artigas, M. Vila, and A. Bortolozzi are authors of the patent WO/2011/131693 issued for the siRNA and ASO molecules and the targeting approach related to this work. R. Revilla is board members of nLife Therapeutics S.L. A. Montefeltro is stockholder of nLife Therapeutics S.L. The rest of authors declare no competing interests.

Author contributions

Conceptualization, A.B.; methodology R.R., A.M., J.H.K., M.V. and A. B.; investigation, D.A-A., R.P-C., V.C-S., L.M-R., A.F-C., E.R-B., M.G., V.P, L.C., R.R., A.M., J.H.K., M.V., F.A. and A.B; writing, A.B.; revisions, D.A-A., R.P-C., V.C-S., L.M-R., A.F-C., E.R-B., M.G., V.P, L.C., R.R., A.M., J.H.K., M.V., F.A. and A.B; visualization, A.B; supervision, A.B., and funding acquisition, F.A., M.V. and A.B.

Additional information

Supplementary material includes statistical information, toxicity studies in mice and six figures.

Supplementary materials

Supplementary material associated with this article can be found, in the online version, at doi:10.1016/j.ebiom.2020.102944.

References

1 Goedert M, Jakes R, Spillantini MG. The synucleinopathies: twenty years on. J Parkinsons Dis 2017;7:S53–71.
2 Polymeropoulos MH, Lavedan C, Leroy E, Ide SE, Dehejia A, Dutra A, et al. Mutation in the a-synuclein gene identified in families with Parkinson's disease. Science 1997;276:2045–7.
3 Spillantini MG, Crowther RA, Jakes R, Hasegawa M, Goedert M. Alpha-Synuclein in filamentous inclusions of Lewy bodies from Parkinson's disease and dementia with Lewy bodies. Proc Natl Acad Sci USA 1998;95:6469–73.
4 Singleton AB, Farrer M, Johnson J, Singleton A, Hague S, Kachergus J, et al. Alpha-synuclein locus triplication causes Parkinson's disease. Science 2003;302:841.
5 Pals P, Lincoln S, Manning J, Heckman M, Skipper L, Hulihan M, et al. Alpha-Synuclein promoter confers susceptibility to Parkinson's disease. Ann Neurol 2004;56:591–5.
6 Domingo A, Klein C. Genetics of Parkinson disease. Handb Clin Neurol 2018;147:211–27.
7 Nalls MA, Pankratz N, Lill CM, Do CB, Hernandez DG, Saad M, et al. Large-scale meta-analysis of genome-wide association data identifies six new risk loci for Parkinson's disease. Nat Genet 2014;46:989–93.
8 Chang D, Nalls MA, Hallgrímsdóttir IB, Hunkapiller J, van der Brug M, Cai F, et al. A meta-analysis of genome-wide association studies identifies 17 new Parkinson's disease risk loci. Nat Genet 2017;49:1511–6.
9 Braak H, Del Tredici K, Rüb U, de Vos RA, Jansen Steur EN, Braak E. Staging of brain pathology related to sporadic Parkinson's disease. Neurobiol Aging 2003;24:197–211.
10 Conway KA, Rochet JC, Bieganski RM, Lansbury PT. Kinetic stabilization of the a-synuclein protofibril by a dopamine-α-synuclein adduct. Science 2001;294:1346–9.
11 Uversky VN. Neuropathology, biochemistry, and biophysics of a-synuclein aggregation. J Neurochem 2007;103:17–37.
12 Dehay B, Bourdenx M, Gorry P, Przedborski S, Vila M, Hunot S, et al. Targeting α-synuclein for treatment of Parkinson's disease: mechanistic and therapeutic considerations. Lancet Neurol 2015;14:855–66.
13 Villar-Piqué A, Lopes da Fonseca T, Outeiro TF. Structure, function and toxicity of alpha-synuclein: the Bermuda triangle in synucleinopathies. J Neurochem 2016;139:240–55.
14 Sardi SP, Cedarbaum JM, Brundin P. Targeted therapies for Parkinson's disease: from genetics to the clinic. Mov Disord 2018;33:684–96.
15 Hayashita-Kinoh H, Yamada M, Yokota T, Mizuno Y, Mochizuki H. Down-regulation of alpha-synuclein expression can rescue dopaminergic cells from cell death in the substantia nigra of Parkinson's disease rat model. Biochem Biophys Res Commun 2006;341:1088–95.
16 Lewis J, Melrose H, Bumcrot D, Hope A, Zehr C, Lincoln S, et al. In vivo silencing of alpha-synuclein using naked siRNA. Mol Neurodegener 2008;3:19.
17 Junn E, Lee KW, Jeong BS, Chan TW, Im JY, Mouradian MM. Repression of alpha-synuclein expression and toxicity by microRNA-7. Proc Natl Acad Sci USA 2009;106:13052–7.
18 McCormack AL, Mak SK, Henderson JM, Bumcrot D, Farrer MJ, Di Monte DA. Alpha-synuclein suppression by targeted small interfering RNA in the primate substantia nigra. PLoS One 2010;5:e12122.
19 Zharikov A, Bai Q, De Miranda BR, Van Laar A, Greenamyre JT, Burton EA. Long-term RNAi knockdown of α-synuclein in the adult rat substantia nigra without neurodegeneration. Neurobiol Dis 2019;125:146–53.
20 Cole T, Paumier K, Zhao H, Weinhofen A, Kordasiewicz H, Swyze E. Snca targeted antisense oligonucleotides mediate progression of pathological deposition in alpha synuclein rodent transmission models of Parkinson's disease. Neurology 2016;86:P6.239.
21 Helmschrodt C, Höbel S, Schöniger S, Bauer A, Bonicelli J, Gringmuth M, et al. Polyethylenimine nanoparticle-mediated siRNA delivery to reduce α-synuclein expression in a model of Parkinson's disease. Mol Ther Nucleic Acids 2017;9:57–68.
22 Nakamori M, Junn E, Mochizuki H, Mouradian MM. Nucleic acid-based therapeutics for Parkinson's disease. Neutherapeutics 2019;16:287.
23 Spencer B, Trinh I, Rockenstein E, Mante M, Florio J, Adame A, et al. Systemic peptide mediated delivery of a siRNA targeting α-synuclein in the CNS ameliorates the neurodegenerative process in a transgenic model of Lewy body disease. Neurobiol Dis 2019;127:163–77.
24 Gorbatyuk OS, Li S, Nash K, Gorbatyuk M, Lewin AS, Sullivan LF, et al. In vivo RNAi-mediated α-synuclein silencing induces nigrostriatal degeneration. Mol Ther 2010;18:1450–7.
25 Khodr CE, Sapru MK, Pedapati J, Han Y, West NC, Kells AP, et al. An α-synuclein AAV gene silencing vector ameliorates a behavioral deficit in a rat model of Parkinson's disease, but displays toxicity in dopamine neurons. Brain Res 2011;1395:94–107.
26 Collier TJ, Redmond Jr DE, Steece-Collier K, Lipton JW, Manfredsson FP. Is alpha-synuclein loss-of-function a contributor to Parkinsonian pathology? evidence from non-human primates. Front Neurosci 2016;10:12.
27 Benskey MJ, Sellnow RC, Sandoval IM, Sortwell CE, Lipton JW, Manfredsson FP. Silencing alpha synuclein in mature nigral neurons results in rapid neuroinflammation and subsequent toxicity. Front Mol Neurosci 2018;11:36.
28 Artigas F, Bortolozzi A. Therapeutic potential of conjugated siRNAs for the treatment of major depressive disorder. Neuropsychopharmacol 2017;42:371.
29 Bortolozzi A, Castañé A, Semakova J, Santana N, Alvarado G, Cortés R, et al. Selective siRNA-mediated suppression of 5-HT1A autoreceptors evokes strong anti-depressant-like effects. Mol Psychiatry 2012;17:612–23.
30 Ferrés-Coy A, Galofré M, Pilar-Cuéllar F, Vidal R, Paz V, Ruiz-Bronchal E, et al. Therapeutic antidepressant potential of a conjugated siRNA silencing the serotonin transporter after intranasal administration. Mol Psychiatry 2016;21:328–38.
31 Alarcón-Arís D, Recasens A, Galofré M, Carballo-Carbajal I, Zacchi N, Ruiz-Bronchal E, et al. Selective α-synuclein knockdown in monoamine neurons by intranasal oligonucleotide delivery: potential therapy for Parkinson's disease. Mol Ther 2018;26:550–67.
32 Fullana MN, Ferrés-Coy A, Ortega JE, Ruiz-Bronchal E, Paz V, Meana JJ, et al. Selective knockdown of TASK3 potassium channel in monoamine neurons: A new therapeutic approach for depression. Mol Neurobiol 2019;56:3038–52.
33 Bernheimer H, Birkmayer W, Hornykiewicz O, Jellinger K, Seitelberger F. Brain dopamine and the syndromes of Parkinson and Huntington. clinical, morphological and neurochemical correlations. J Neurol Sci 1973;20:415–55.
34 Kish SJ, Shannak K, Hornykiewicz O. Uneven pattern of dopamine loss in the striatum of patients with idiopathic Parkinson's disease. pathophysiologic and clinical implications. N Engl J Med 1988;318:876–80.
35 Fearnley JM, Lees AJ. Ageing and Parkinson's disease: substantia nigra regional selectivity. Brain 1991;114:2283–301.
36 Chu Y, Kordower JH. Age-associated increases of alpha-synuclein in monkeys and humans are associated with nigrostriatal dopamine depletion: Is this the target for Parkinson's disease? Neurobiol Dis 2007;25:134–49.
37 Mak MK, Pang MY. Fear of falling is independently associated with recurrent falls in patients with Parkinson's disease: a 1-year prospective study. J Neurol 2009;256:1689–95.

38 Tong J, Wong H, Guttman M, Ang LC, Forno LS, Shimadzu M, et al. Brain alpha-synuclein accumulation in multiple system atrophy, Parkinson's disease and progressive supranuclear palsy: a comparative investigation. Brain 2010;133:172–88.
39 Kirik D, Rosenblad C, Burger C, Lundberg C, Johansen TE, Muzyczka N, et al. Parkinson-like neurodegeneration induced by targeted overexpression of alpha-synuclein in the nigrostriatal system. J Neurosci 2002;22:2780–91.
40 Franklin KBJ, Paxinos G. The Mouse Brain in Stereotaxic Coordinates. New York, USA: Elsevier Academic Press; 2008.
41 Torra A, Parent A, Cuadros T, Rodríguez-Galván B, Ruiz-Bronchal E, Ballabio A, et al. Overexpression of TFEB drives a pleiotropic neurotrophic effect and prevents Parkinson's disease-related neurodegeneration. Mol Therapy 2018;26:1552–67.
42 Carballo-Carbajal I, Laguna A, Romero-Giménez J, Cuadros T, Bové J, Martinez-Vicente M, et al. Brain tyrosinase overexpression implicates age-dependent neuromelanin production in Parkinson's disease pathogenesis. Nat Commun 2019;10:973.
43 Li CH, Tam PKS. An alternative algorithm for minimum cross entropy thresholding. Pattern Recognit Let 1998;19:771–6.
44 Otsu N. A threshold selection method from gray-level histograms. IEEE Trans Syst Man Cybern 1979;9:62–6.
45 Kapur JN, Sahoo PK, Wong ACK. A new method for gray-level picture thresholding using the entropy of the histogram. Graph Models Image Process 1985;29:273–85.
46 Lassen LB, Gregersen E, Isager AK, Betzer C, Kofoed RH, Jensen PH. ELISA method to detect a-synuclein oligomers in cell and animal models. PLoS One 2018;13:e0196056.
47 Ludtmann MHR, Angelova PR, Horrocks MH, Choi ML, Rodrigues M, Baev AY, et al. α-Synuclein oligomers interact with ATP synthase and open the permeability transition pore in Parkinson's disease. Nat Commun 2018;9:2293.
48 Park HY, Ryu YK, Go J, Son E, Kim KS, Kim MR. Palmitoyl serotonin inhibits L-dopa-induced abnormal involuntary movements in the mouse Parkinson model. Exp Neurobiol 2016;25:174–84.
49 Marazziti D, Golini E, Mandillo S, Magrelli A, Witke W, Matteoni R, et al. Altered dopamine signaling and MPTP resistance in mice lacking the Parkinson's disease-associated GPR37/parkin-associated endothelin-like receptor. Proc Natl Acad Sci USA 2004;101:10189–94.
50 Kokhan VS, Van'kin GI, Bachurin SO, Shamakina IY. Differential involvement of the gamma-synuclein in cognitive abilities on the model of knockout mice. BMC Neurosci 2013;14:53.
51 Fujiwara H, Hasegawa M, Dohmae N, Kawashima A, Masliah E, Goldberg MS, et al. α-Synuclein is phosphorylated in synucleinopathy lesions. Nat Cell Biol 2002;4:160–4.
52 Yamada M, Iwatsubo T, Mizuno Y, Mochizuki H. Overexpression of alpha-synuclein in rat substantia nigra results in loss of dopaminergic neurons, phosphorylation of alpha-synuclein and activation of caspase-9: resemblance to pathogenetic changes in Parkinson's disease. J Neurochem 2004;91:451–61.
53 Andersson DR, Nissbrandt H, Bergquist F. Partial depletion of dopamine in substantia nigra impairs motor performance without altering striatal dopamine neurotransmission. Eur J Neurosci 2006;24:617–24.
54 Brown MW, Aggleton JP. Recognition memory: what are the roles of the perirhinal cortex and hippocampus? Nat Rev Neurosci 2001;2:51–61.
55 Winters BD, Forwood SE, Cowell RA, Saksida LM, Bussey TJ. Double dissociation between the effects of peri-postrhinal cortex and hippocampal lesions on tests of object recognition and spatial memory: heterogeneity of function within the temporal lobe. J Neurosci 2004;24:5901–8.
56 Maingay M, Romero-Ramos M, Carta M, Kirik D. Ventral tegmental area dopamine neurons are resistant to human mutant alpha-synuclein overexpression. Neurobiol Dis 2006;23:522–32.
57 Phillipson OT, Kilpatrick IC, Jones MW. Dopaminergic innervation of the primary visual cortex in the rat, and some correlations with human cortex. Brain Res Bull 1987;18:621–33.
58 Berger B, Gaspar P, Verney C. Dopaminergic innervation of the cerebral cortex: unexpected differences between rodents and primates. Trends Neurosci 1991;14:21–7.
59 Molochnikov I, Cohen D. Hemispheric differences in the mesostriatal dopaminergic system. Front Syst Neurosci 2014;8:110.
60 Nemani VM, Lu W, Berge V, Nakamura K, Onoa B, Lee MK, et al. Increased expression of alpha-synuclein reduces neurotransmitter release by inhibiting synaptic vesicle reclustering after endocytosis. Neuron 2010;65:66–79.
61 Lengyel K, Pieschl R, Strong T, Molski T, Mattson G, Lodge NJ, et al. Ex vivo assessment of binding site occupancy of monoamine reuptake inhibitors: methodology and biological significance. Neuropharmacol 2008;55:63–70.
62 Smith RA, Miller TM, Yamanaka K, Monia BP, Condon TP, Hung G, et al. Antisense oligonucleotide therapy for neurodegenerative disease. J Clin Invest 2006;116:2290–6.
63 Kordasiewicz HB, Stanek LM, Wancewicz EV, Mazur C, McAlonis MM, Pytel KA, et al. Sustained therapeutic reversal of Huntington's disease by transient repression of huntingtin synthesis. Neuron 2012;74:1031–44.
64 Dhuria SV, Hanson LR, Frey WH. Intranasal delivery to the central nervous system: mechanisms and experimental considerations. J Pharm Sci 2010;99:1654–73.
65 Lochhead JJ, Thorne RG. Intranasal delivery of biologics to the central nervous system. Adv Drug Deliv Rev 2012;64:614–28.
66 Takahashi M, Suzuki M, Fukuoka M, Fujikake N, Watanabe S, Murata M, et al. Normalization of overexpressed alpha-synuclein causing Parkinson's disease by a moderate gene silencing with RNA interference. Mol Ther Nucleic Acids 2015;4:e241.
67 Jiang J, Zhu Q, Gendron TF, Saberi S, McAlonis-Downes M, Seelman A, et al. Gain of toxicity from ALS/FTD-linked repeat expansions in C9ORF72 is alleviated by antisense oligonucleotides targeting GGGGCC-containing RNAs. Neuron 2016;90:535–50.
68 Scoles DR, Meera P, Schneider MD, Paul S, Dansithong W, Figueroa KP, et al. Antisense oligonucleotide therapy for spinocerebellar ataxia type 2. Nature 2017;544:362–6.
69 Smith CIE, Zain R. Therapeutic oligonucleotides: State of the art. Annu Rev Pharmacol Toxicol 2019;59:605–30.
70 Hardee CL, Arévalo-Soliz LM, Hornstein BD, Zechiedrich L. Advances in non-viral DNA vectors for gene therapy. Genes (Basel) 2017;8:E65.
71 Nyamay'Antu A, Dumont M, Kedinger V, Erbacher V. Non-Viral vector mediated gene delivery: the outsider to watch out for in gene therapy. Cell Gene Ther Insights 2019;5:51–7.
72 Schoch KM, Miller TM. Antisense oligonucleotides: Translation from mouse models to human neurodegenerative diseases. Neuron 2017;94:1056–70.
73 Winner B, Jappelli R, Maji SK, Desplats PA, Boyer L, Aigner S, et al. In vivo demonstration that alpha-synuclein oligomers are toxic. Proc Natl Acad Sci USA 2011;108:4194–9.
74 Volpicelli-Daley LA, Kirik D, Stoyka LE, Standaert DG, Harms AS. How can rAAV-α-synuclein and the fibril α-synuclein models advance our understanding of Parkinson's disease? J Neurochem 2016(Suppl 1):131–55.
75 Yamada M, Iwatsubo T, Mizuno Y, Mochizuki H. Overexpression of alpha-synuclein in rat substantia nigra results in loss of dopaminergic neurons, phosphorylation of alpha-synuclein and activation of caspase-9: resemblance to pathogenetic changes in Parkinson's disease. J Neurochem 2004;91:451–61.
76 Taymans JM, Vandenberghe LH, Haute CV, Thiry I, Deroose CM, Mortelmans L, et al. Comparative analysis of adeno-associated viral vector serotypes 1, 2, 5, 7, and 8 in mouse brain. Hum Gene Ther 2007;18:195–6.
77 Lundblad M, Decressac M, Mattsson B, Bjorklund A. Impaired neurotransmission caused by overexpression of alpha-synuclein in nigral dopamine neurons. Proc Natl Acad Sci USA 2012;109:3213–9.
78 Henrich MT, Geibl FF, Lee B, Chiu WH, Koprich JB, Brotchie JM, et al. A53T-α-synuclein overexpression in murine locus coeruleus induces Parkinson's disease-like pathology in neurons and glia. Acta Neuropathol Commun 2018;6:39.
79 Halliday GM, Blumbergs PC, Cotton RG, Blessing WW, Geffen LB. Loss of brainstem serotonin- and substance P-containing neurons in Parkinson's disease. Brain Res 1990;510:104–7.
80 Bertrand E, Lechowicz W, Szpak GM, Dymecki J. Qualitative and quantitative analysis of locus coeruleus neurons in Parkinson's disease. Folia Neuropathol 1997;35:80–6.
81 Kish SJ, Tong J, Hornykiewicz O, Rajput A, Chang LJ, Guttman M, et al. Preferential loss of serotonin markers in caudate versus putamen in Parkinson's disease. Brain 2008;131:120–31.
82 Politis M, Wu K, Loane C, Quinn NP, Brooks DJ, Oertel WH, et al. Serotonin neuron loss and nonmotor symptoms continue in Parkinson's patients treated with dopamine grafts. Sci Transl Med 2012;4:128ra41.
83 McBride JL, Pitzer MR, Boudreau RL, Dufour B, Hobbs T, Ojeda SR, et al. Preclinical safety of RNAi-mediated HTT suppression in the rhesus macaque as a potential therapy for Huntington's disease. Mol Ther 2011;19:2152–62.